AWARD NUMBER: W81XWH-16-1-0133

TITLE: Elastomeric Auxetic Urogential Meshes: Exploring Alternatives to Knitted Polypropylene

PRINCIPAL INVESTIGATOR: Dr. Pamela Moalli

CONTRACTING ORGANIZATION: Magee-Womens Research Institute and Foundation

REPORT DATE: Jan 2020

TYPE OF REPORT: Final

PREPARED FOR: U.S. Army Medical Research and Materiel Command
Fort Detrick, Maryland 21702-5012

REPORT DOCUMENTATION PAGE

Form Approved
OMB No. 0704-0188

1. REPORT DATE	2. REPORT TYPE	3. DATES COVERED
Jan 2020	Final	09/30/2016 - 09/29/2019

4. TITLE AND SUBTITLE

Elastomeric Auxetic Urogential Meshes: Exploring Alternatives to Knitted Polypropylene

5a. CONTRACT NUMBER

5b. GRANT NUMBER
W81XWH-16-1-0133

5c. PROGRAM ELEMENT NUMBER

6. AUTHOR(S)

Pamela Moalli
Steve Abramowitch
Rui Liang

E-Mail: moalpa@mail.magee.edu

5d. PROJECT NUMBER

5e. TASK NUMBER

5f. WORK UNIT NUMBER

7. PERFORMING ORGANIZATION NAME(S) AND ADDRESS(ES)

Magee-Womens Research Institute and Foundation
3339 Ward Street
Pittsburgh, PA 15213-4430

8. PERFORMING ORGANIZATION REPORT NUMBER

9. SPONSORING / MONITORING AGENCY NAME(S) AND ADDRESS(ES)

U.S. Army Medical Research and Materiel Command
Fort Detrick, Maryland 21702-5012

10. SPONSOR/MONITOR'S ACRONYM(S)

USAMRAA

11. SPONSOR/MONITOR'S REPORT NUMBER(S)

12. DISTRIBUTION / AVAILABILITY STATEMENT

Approved for Public Release; Distribution Unlimited

13. SUPPLEMENTARY NOTES

14. ABSTRACT

We developed novel synthetic prolapse meshes based on auxetic pore geometries (ie the pores expand rather than contract when loaded) manufactured from soft elastomers (polydimethysiloxane, PDMS, and polycarbonate urethane, PCU). This is contrary to current polypropylene meshes in which the pores collapse with loading and they are manufactured from stiff polypropylene. The purpose of this study was to test the hypothesis that the novel elastomeric, auxetic prolapse meshes will evoke improved tissue integration and preserve vaginal function relative to current commonly used polypropylene prolapse meshes. To test this hypothesis, we developed and validated a rabbit model for implanting mesh onto the internal vagina of a rabbit via a lumbar colpopexy. Furthermore, we were able to reproduce one of the most common mesh complications - a mesh exposure corroborating the utility of the rabbit as a model for understanding mesh complications. Following implantation for 3 months onto the rabbit vagina, the PDMS mesh had the least negative impact on the vagina. The PCU mesh impacted the rabbit vagina similar to Restorelle. Collectively, these results suggest that the host response to mesh is more sensitive to the polymer and further optimization of the design of the mesh is warranted. The results of this study were used as preliminary data in an NIH R01 application which was successfully funded in February 2019 (NICHD R01 HD097187). Additionally, the results of this study were published in two peer-reviewed manuscripts (a third manuscript is in preparation) and discussed in over 20 scientific local and national meetings/seminars/conferences.

15. SUBJECT TERMS

prolapse, auxetic, pore, porosity, elastomer

16. SECURITY CLASSIFICATION OF:			17. LIMITATION OF ABSTRACT	18. NUMBER OF PAGES	19a. NAME OF RESPONSIBLE PERSON
a. REPORT	b. ABSTRACT	c. THIS PAGE			USAMRMC
Unclassified	Unclassified	Unclassified	Unclassified	45 excl. TOC & Cover	19b. TELEPHONE NUMBER *(include area code)*

Table of Contents

Page

1. INTRODUCTION:

Roughly 300,000 surgeries are performed annually in the US to repair pelvic organ prolapse (POP) – a common condition in women in which the pelvic organs descend into the vaginal lumen. The changing demographics of the VA population with more women utilizing VA benefits and services combined with the increased risk of developing POP in women engaging in strenuous activity portends a rapidly escalating demand for repair of POP and related conditions among female veterans. Following POP surgical repairs utilizing a woman's own tissues, 40% will fail by 2 years, and 70% by 4 years prompting surgeons to seek materials to augment repairs, most commonly polypropylene mesh. While current literature supports the use of knitted, lightweight, wide pore polypropylene, the ideal mesh has not been defined and no mesh to date is without complications.

Currently, all meshes used in POP repairs are hernia meshes simply remarketed as 510K devices for a different indication. Hernia meshes are comprised of a stiff plastically deforming polymer (polypropylene), whose use prior to 2011 was motivated by the need for mesh products to be similar to their abdominal hernia counterparts so that a 510K device status could be retained. Thus, prolapse meshes were never developed specifically for the mechanical and physiologic needs of the vagina and polypropylene was never deemed the ideal polymer. In addition, for hernia repairs, large pores (>1mm) have been shown to be critical for successful host tissue integration. Yet, recent research has revealed that when implanted for POP repairs, unlike in the abdominal wall, polypropylene mesh pores are much more likely to collapse below the critical 1 mm threshold. Pore collapse leads to localized areas of increased mesh burden (density) and altered mesh mechanics (increased stiffness) increasing the risk of complications, particularly pain and mesh erosion/exposure.

In response to the Department of Defense Discovery Award in the Program Topic Area "Advanced Prosthetics", we propose to develop a novel synthetic prolapse mesh based on an auxetic pore geometry that 1) undergoes elastic as opposed to plastic deformation and 2) maintains or exceeds its initial pore sizes when loaded, with 3) a material stiffness that matches that of the vagina. An "auxetic" structure is one that has a negative Poisson's ratio. Thus, instead of the middle of the device collapsing in on itself when placed in tension, as in most current polypropylene meshes, the middle expands leading to increased pore sizes with mechanical loading. The meshes will be constructed using elastomeric polymers. Unlike polypropylene, these meshes will extend and contract as they are loaded and unloaded respectively; thereby behaving more similar to native supportive tissues. **We hypothesize that these novel elastomeric, auxetic prolapse meshes will evoke improved tissue integration and preserve vaginal function relative to current commonly used polypropylene prolapse meshes.**

2. KEYWORDS: prolapse, auxetic, pore, porosity, elastomer

3. ACCOMPLISHMENTS:

What were the major goals of the project?

Aim 1: To utilize computational modeling to design and then construct a novel device that affords sufficient anatomic support to the vagina and hence the pelvic organs while maximizing device porosity

- Conduct computational modeling of a prototype device

    - Milestone achieved: prototypes of polydimethylsiloxane (PDMS) and polycarbonate (PCU) obtained – completed
    - Milestone achieved: IACUC Approval – completed
    - Milestone achieved: paper accepted – completed (see list of Journal publications)
- Manufacture prototype devices
    - Milestone achieved: elastomeric auxetic devices created and the mechanical behavior described – completed
    - Milestone achieved: paper accepted – in progress (mechanics of prototypes will be included with the *in vivo* paper, Aim 3)

Aim 2: To develop and validate the rabbit model for mesh implantation

- Compare rabbit and nonhuman primate host response following implantation of Restorelle (commercially available mesh)
    - Milestone achieved: abstract submission to national meeting – completed
    - Milestone achieved: paper accepted – completed

Aim 3: To evaluate the host response to an elastomeric auxetic mesh and to compare this response to a commercially available polypropylene mesh, Restorelle

- Implant prototype devices
    - Milestone achieved: characterization of the host response to a novel elastomeric auxetic mesh – completed
    - Milestone achieved: paper accepted – paper in progress

What was accomplished under these goals?

Aim 1: Computational modeling and mechanical testing demonstrated that the bowtie auxetic geometry is the most favorable geometry given that the pores of the bowtie model expanded and maintained auxetic behavior at increasing loads with the least amount of model deformation and limited elongation, ~30% (See publication: Knight et al 2018, Preventing Mesh Pore Collapse by Designing Mesh Pores With Auxetic Geometries: A Comprehensive Evaluation, Journal of Biomechanical Engineering). Based on these results, a novel elastomeric auxetic mesh using the bowtie geometry was manufactured from polydimethylsiloxane (PDMS) and polycarbonate urethane (PCU). The material stiffness of PDMS and PCU utilized were both on the same order of magnitude as vaginal tissue (PDMS material stiffness = 10 MPa, PCU material stiffness = 27 MPa, vaginal stiffness = 6-14 MPa (human) and 25-34 MPa (animal)). Uniaxial tensile testing was used to determine the structural properties of the two meshes (Table 1).

Table 1: Uniaxial structural properties of the PDMS and PCU meshes.

	PDMS (n=5)	PCU (n=5)
Low Stiffness (N/mm)	0.06 ± 0.01	0.09 ± 0.01
High Stiffness (N/mm)	0.12 ± 0.01	0.20 ± 0.01
Ultimate Load (N)	4.77 ± 0.62	20.87 ± 1.65
Relative Elongation (mm/mm)	0.51 ± 0.01	0.52 ± 0.01
Energy Absorbed (N*mm)	115.3 ± 24.1	1926 ± 265

Data represented as mean ± standard deviation.

Aim 2: We developed a novel method to implant mesh onto the internal rabbit vagina via a lumbar colpopexy. Comparable to what we found in nonhuman primates (NHPs), polypropylene mesh had a negative impact on vaginal smooth muscle function in the rabbit with a 43% decrease in vaginal contractility following the implantation of Restorelle (Figure 1). Vaginal contractility decreased by 46% in the NHP following the implantation of Restorelle (Feola et al 2013). The observed decrease in contractile function was also associated with an 18% reduction in the rabbit vaginal smooth muscle layer (Figure 2). Thinning of the vaginal smooth muscle layer in the NHP was also observed previously (Liang et al 2013). Additionally, we observed mesh buckling with the implantation of Restorelle on the rabbit vagina, in spite our efforts to implant the mesh in a flat configuration. In the areas where the mesh buckled, the underlying vagina was significantly thinned – characteristic of a mesh exposure (Figure 2). Collectively these results suggest that not

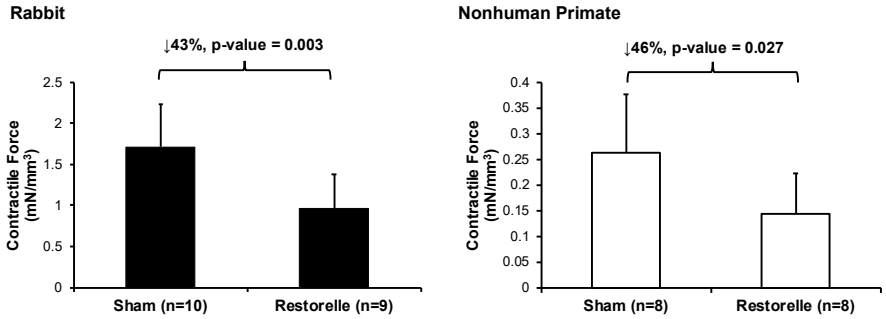

Figure 1: Contractile force of the rabbit (left) and nonhuman primate (right) vagina in response to 120 mM KCl. The contractile force of the rabbit vagina significantly decreased by 43% with the implantation of Restorelle via a lumbar colpopoexy and this result is similar to the 46% decrease in contractility with the implantation of Restorelle onto the nonhuman primate vagina via an abdominal sacral colpopexy.

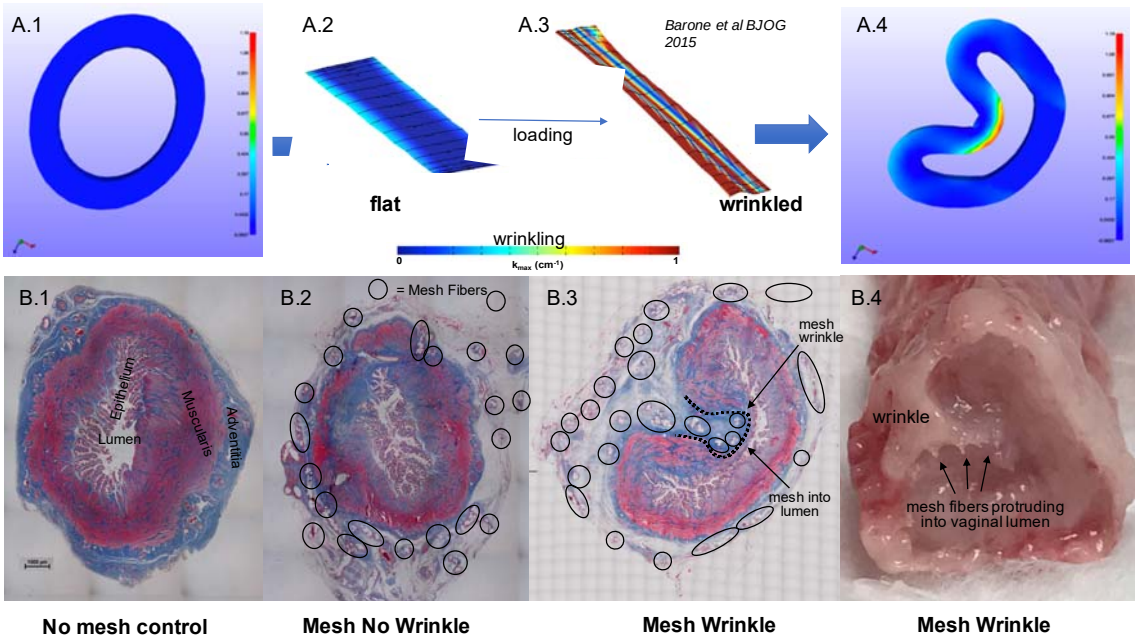

Figure 2. Mesh wrinkling and impact on the vagina after implantation by sacrocolpopexy in the rabbit. A.1 is a modeled cross-section of the vaginal muscularis. A.2-3 show a 3D image of mesh and corresponding surface curvature K_{max} with loading. Tensioning/loading mesh can cause wrinkling which pushes in on the vagina as shown in the shape (A.4) with corresponding cross-section and gross anatomy (below, B.3-4). Computational analysis (upper panel) deforming the geometry on the left (A.1) into the geometry on the right (A.4)reveals a strain distribution that is consistent with what would be predicted from a simple beam analysis. In the cross section image of a mesh wrinkle (B.3), locations where curvature and tissue strain are the highest corresponds to where the vaginal vaginal wall (especially smooth muscle) has thinned to the point where mesh fibers (circled in black) enter into the lumen of the vagina (mesh exposure). The is in contrast to the middle image (B) where mesh was implanted flat without wrinkles leading to general smooth muscle thinning relative to control, but no regions where mesh fibers are close to the lumen of the vagina. Thus, these data show that mesh wrinkling should be avoided, which one of the major focuses of this proposal.

only is the rabbit a valid model for testing the host response to mesh, but it is also useful for understanding mechanisms of one of the most common mesh complications – a mesh exposure.

Table 2: Maximum vaginal contractile force in response to 120 mM KCl, Electrical Field Stimulation, and Phenylephrine.

	120 mM KCl (mN/mm^3)	Electrical Field Stimulation (g/g)	Phenylephrine (g/g)
Sham (n=10)	1.71 ± 0.52	0.46 (0.69)	1.50 (0.36)
Restorelle (n=9)	1.13 ± 0.50	0.51 (0.42)	1.26 (0.67)
PDMS (n=9)	1.44 ± 0.38	0.66 (0.27)	1.10 (0.70)
PCU (n=8)	0.83 ± 0.28	0.40 (0.16)	0.29 (1.02)
Overall p-value	0.001[a]	0.142[b]	0.010[b]
Sham vs Restorelle	0.036	N/A	N/A
Sham vs PDMS	0.660	N/A	N/A
Sham vs PCU	0.001	N/A	0.002
Restorelle vs PDMS	0.591	N/A	N/A
Restorelle vs PCU	0.660	N/A	0.054
PDMS vs PCU	0.044	N/A	0.034

Data represented as mean ± standard deviation and median (interquartile range).
[a]Overall p-value obtained using One-way ANOVA followed by Gabriel's pairwise post-hoc test.
[b]Overall p-value obtained using Kruskal-Wallis followed by Mann-Whitney test with a Bonferroni correction with significance set to p-value < 0.0167.

Aim 3: The elastomeric auxetic meshes developed and manufactured in Aim 1, were implanted onto the vagina of 20 New Zealand White Rabbits (PDMS n = 10 and PCU n=10) via a lumbar colpopexy for 12-weeks. For comparison, Restorelle (polypropylene mesh, n=10) was also implanted. Ten animals served as Sham, no mesh implanted. After 12-weeks, the mesh-vagina complexes were explanted and the contractile function of the vagina (active mechanics), smooth muscle morphology and thickness, collagen structure, total collagen and sulphated glycosaminoglycan (GAG) content, and foreign body response were assessed.

For the active mechanics, a vaginal contractility assay was performed in which the mesh-vagina complexes or vagina alone in the case of Sham were exposed to 3 stimuli in order to assess the contractile function of the vagina (an indirect measure of the contractile function of the vaginal smooth muscle): 120 mM KCl (assesses muscle-mediated contractions), electrical field stimulation - 20 V for a duration of 5 secs and the frequency was increased from 1-64 Hz (assesses nerve-mediated contractions), and 10^{-7} to 10^{-4} M phenylephrine (an α_1-adreno-receptor agonist), applied non-cumulatively (assesses receptor-mediated contractions). In response to 120 mM KCl, the contractile force of the vagina was significantly decreased with the implantation of Restorelle (p-value = 0.036) and PCU (p-value = 0.001) relative to Sham (Table 2). There were no significant differences in the contractile response to electrical field stimulation, p-value = 0.142. The contractile force in response to phenylephrine stimulation for the PCU implanted vaginas was significantly less than Sham (p-value = 0.002). Overall, good tissue ingrowth between the pores was observed for all meshes (Figure 3).

Table 3: Total collagen content and sulphated glycosaminoglycan content following 12-week implantation of Restorelle, PDMS, and PCU meshes.

	Total Collagen Content (% tissue dry weight)	Sulphated Gylcosaminoglycan Content (% tissue dry weight)
Sham (n=10)	36.5 ± 7.8	1.8 ± 0.2
Restorelle (n=7)	17.1 ± 6.1	0.7 ± 0.2
PDMS (n=9)	23.8 ± 8.4	1.0 ± 0.3
PCU (n=8)	16.4 ± 3.9	0.7 ± 0.2
Overall p-value	< 0.001[a]	< 0.001[a]
Sham vs Restorelle	< 0.001	< 0.001
Sham vs PDMS	0.002	< 0.001
Sham vs PCU	< 0.001	< 0.001
Restorelle vs PDMS	0.307	0.130
Restorelle vs PCU	1.000	1.000
PDMS vs PCU	0.189	0.170

Data represented as mean ± standard deviation and median (interquartile range).
[a]Overall p-value obtained using One-way ANOVA followed by Gabriel's pairwise post-hoc test.

Compared to Restorelle, the PDMS and PCU meshes had a markedly reduced macrophage response (Figure 3). Relative to Sham, total collagen and GAG content were both significantly decreased with the implantation of all meshes (Table 3). There were no significant differences in the collagen and GAG content between the mesh implanted vaginas.

Overall, the meshes manufactured from the softest elastomer, PDMS, preserved vaginal smooth muscle function and had less of a negative impact on the vagina compared to the PCU and Restorelle meshes. The impact of the PCU mesh on vaginal structure and function was similar to Restorelle and this is likely a result of the PCU mesh being structurally too stiff. Nonetheless, these results demonstrate the potential of manufacturing meshes from a soft elastomer to improve the impact of the mesh on the vagina. The PDMS mesh manufactured in this study, is not strong enough to withstand the loads in the female pelvis, yet PCU is strong enough. In future studies (newly funded NIH grant, see Major Accomplishment Section), we will work to optimize the design of the PCU mesh such that the impact of the newly designed PCU mesh on the vagina matches, ideally it will exceed, that of Restorelle.

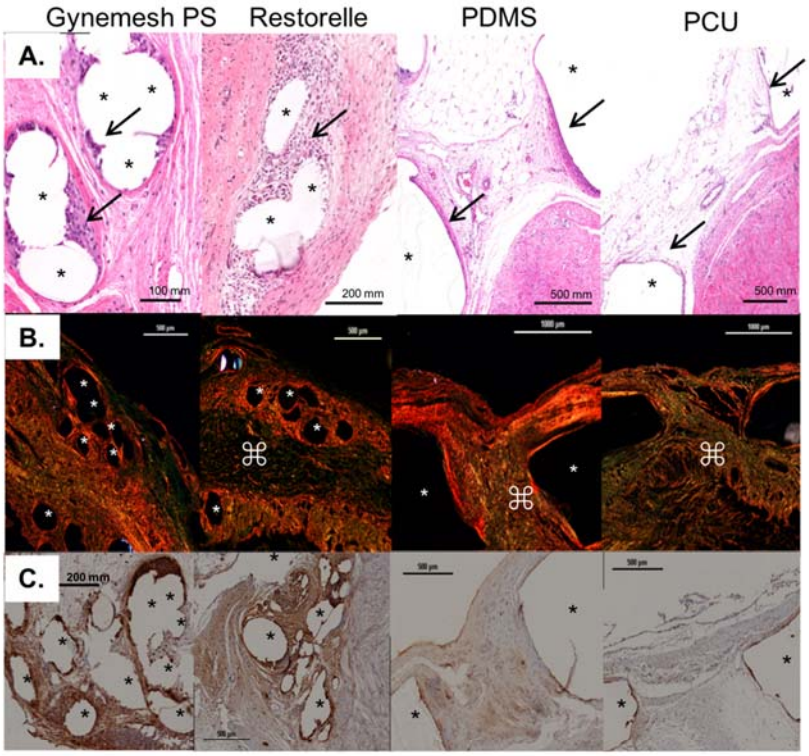

Figure 3. Host response at 3mos after implantation of polypropylene meshes Gynemesh and Restorelle vs EAMs - PDMS and PCU. A. Limited foreign body response (arrow) to the fibers (*) is seen in EAMs as compared to polypropylene meshes. B. Picrosirius red staining confirms presence of thick red collagen fibers (capsule) around Gynemesh (⌘) PS with no normal tissue between pores (⌘) vs good tissue ingrowth in Restorelle and EAMs with green thin fibers and minimal fibrous capsule observed for PCU. C. Labeling with panmacrophage marker (RAM 11) shows markedly reduced macrophage response (brown stain) for the EAMs as compared to polypropylene.

Major Accomplishment – The results were used as preliminary data in an NIH R01 application which was successfully funded in February 2019 (NICHD R01 HD097187).

What opportunities for training and professional development has the project provided?

1. Katrina Knight: Magee-Womens Research Institute and Foundation Postdoctoral Fellow in the Department of Obstetrics, Gynecology, and Reproductive Sciences at the University of Pittsburgh. Project title: Development of a novel urogynecologic mesh to overcome current limitations of polypropylene. Dr. Knight through this grant enhanced her surgical skills, aided with the development of the rabbit model for this study, and completed the majority of the experiments in this study, which she will disseminate in 3 manuscripts. Currently, Dr. Knight has two first author manuscripts as a result of her work on this study, and is currently working on a third. Additionally, Dr. Knight has presented the work from this study in multiple settings including the annual scientific meeting of the American Urogynecologic Society (AUGS) which has increased her visibility and enhanced her presentations skills.

2. Aimon Iftikhar: Current Ph.D. Candidate in Bioengineering at University of Pittsburgh; NIH TL1 Clinical & Translational Science Predoctoral Fellow Thesis Title: Development of a Clinically Relevant Rabbit Surgical Model of Pelvic Reconstruction to Evaluate the Immune Response to Novel Surgical Materials. She is currently testing a cytokine local delivery system and working on developing the rabbit model for use in this study and also presented at AUGS.

How were the results disseminated to communities of interest?

Annual Scientific Meetings:

- American Urogynecologic Society
- Society for Pelvic Research
- Invited Talks
    - Invited Speaker: Society of Women in Urology (SWIU) 6th Annual Meeting “The science behind the mesh: Fact vs fiction”; Fort Lauderdale, FL -> January 2017
    - Duke University Department of Obstetrics and Gynecology Grand Rounds, “Urogynecologic Mesh Complications: what is the science telling us?” -> June 2017
    - Invited Member of POP & Incontinence Workgroup: “National Women’s Health Technologies Coordinated Registry Network (CRN) Think-Tank”, collaboration between the FDA, the National Institute of Health (NIH)/National Library of Medicine (NLM), the Office of the National Coordinator for Health Information Technology (ONC), the American Congress of Obstetricians and Gynecologists (ACOG), American Urogynecologic Society (AUGS), clinicians, industry and other stakeholders, Silver Spring, MD -> September 2017
    - Invited Speaker: The Royal Society of Science Meeting, London, England “Towards rebuilding vaginal support utilizing an extracellular matrix bioscaffold” -> October 2017
    - Invited Speaker: Endowed David Nichols, MD lectureship, Grand Rounds, Womens & Infants Hospital, Providence, RI, “The science behind urogynecologic meshes: learning from current products to improve future materials” -> November 2017
    - Invited Speaker: Reproductive Sciences Seminars, University of Colorado, Aurora, CO, "The Science Behind Urogynecologic Meshes: Learning from Current Products to Improve Future Materials" -> March 2018

    - Invited Speaker: American Urogynecology Society Basic Science Symposium, Chicago, IL, “The Role of Mechanics in Mesh Complications” -> October 2018
    - Invited Speaker: Grand Rounds, St. Louis University School of Medicine, St. Louis, MO, “Urogynecologic Meshes: A lesson in the evaluation of novel gynecologic devices” -> January 2019
    - Invited Speaker: Howard Kelly Lectureship in Pelvic Reconstructive Surgery, John Hopkins University School of Medicine, Baltimore, MD, “The Science Behind Urogynecologic Meshes: Learning From Current Products to Improve Future Materials” -> April 2019
    - Invited Speaker: 16th International Symposium on Computer Methods in Biomechanics and Biomedical Engineering and 4th Conference on Imaging and Visualization, New York City, NY, “Computer Methods for Understanding and Repair of Pelvic Organ Prolapse” -> August 2019
    - Invited Speaker: Biomedical Engineering Society 2019 Annual Meeting, Philadelphia, PA, “Translational Biomechanics Laboratory: Focus on Pelvic Floor Biomechanics” -> October 2019
    - Invited Speaker: State of the Art Speaker, 4th Annual Meeting of the Society for Pelvic Research, Charleston, SC, “Innovation in Urogynecologic Surgery: A Lesson in the Development of Novel Surgical Biomaterials” -> November 2019
- Local Meetings: Magee-Womens Research Institute Works-in-Progress Seminar Series
    - Knight KM. Development of an Elastomeric Auxetic Mesh for Prolapse Repair: An Alternative to Polypropylene Mesh. Magee-Womens Research Institute Works-in-Progress Seminar Series, Pittsburgh, PA -> November 2017
    - Abramowitch SD. Opportunities for Biomechanics, Tissue Injury, and Rehabilitation Research in Obstetrics and Gynecology. Biomechanics in Regenerative Medicine (BiRM), University of Pittsburgh, Pittsburgh, PA -> July 2019
    - Abramowitch SD. Exposing Pelvic Floor Disorders Using Biomechanics, Image Analysis, and Computer Methods. Biomedical Engineering Seminar, Duquesne University, Pittsburgh, PA -> November 2019
    - Abramowitch SD. Translational Engineering: Novel Insights into Pelvic Floor Disorders and Repair. REI Conference, Pittsburgh, PA -> December 2019

What do you plan to do during the next reporting period to accomplish the goals?

Nothing to Report

4. IMPACT:

What was the impact on the development of the principal discipline(s) of the project?

The development of this product has significantly impacted the Urogynecologic and Pelvic Reconstructive Surgery Community as surgeons are very interested in novel materials that overcome the limitations of polypropylene mesh. Furthermore, with the FDA mandating that manufacturers of transvaginal meshes stop distributing their meshes preceded by a broader ban of the distribution of transvaginal meshes by institutions world-wide, the current project which investigates alternative materials and a novel mesh design has proved to be timely.

What was the impact on other disciplines?

Once the device is tested in large animals, we predict that it will be highly applicable to other disciplines that utilize mesh including general (abdominal and inguinal hernia repair) and thoracic surgery (diaphragmatic hernia repair).

What was the impact on technology transfer?

None to date although we anticipate filing patent rights over the next several months. We have had a long process of working with the DOD to release the technology.

What was the impact on society beyond science and technology?

None to date although anticipate impacting the lives of women with prolapse and incontinence including military women.

5. CHANGES/PROBLEMS:

Changes in approach and reasons for change – Although we initially proposed to use poly(vinyl) alcohol (PVA) as one of the elastomers, we found that it was microporous at the microscopic level – a property that would increase susceptibility to harboring bacteria and becoming infected. Additionally, the manufacturing process needed to develop a mesh as well as the lack of mechanical strength of PVA ultimately led us to consider other elastomers. We also added another Aim in order to validate the appropriateness of using the rabbit model for mesh implantation.

Actual or anticipated problems or delays and actions or plans to resolve them – Working with Kenneth Gall, a material scientist at Duke University, we replaced PVA with a tougher elastomer, polycarbonate urethane. Switching to a new polymer resulted in a delay in animal implantations; however, given the no cost extensions, we were able to complete all animal implantations and experimental endpoints.

Changes that had a significant impact on expenditures – Nothing to Report

Significant changes in use or care of human subjects, vertebrate animals, biohazards, and/or select agents – Nothing to Report

Significant changes in use or care of human subjects – Nothing to Report

Significant changes in use or care of vertebrate animals – Nothing to Report

Significant changes in use of biohazards and/or select agents – Nothing to Report

6. PRODUCTS:

Publications, conference papers, and presentations

Journal publications:

1. Knight KM., Moalli PA., Abramowitch SD. Preventing Mesh Pore Collapse by Designing Mesh Pores with Auxetic Geometries: A Comprehensive Evaluation via Computational Modeling.

Journal of Biomechanical Engineering 2018;140(5):051005-1-051005-8 (accepted and yes acknowledgement of federal support was made)

2. Knight KM., Artsen AM., Routzong MR., King GE., Abramowitch SD., Moalli PA. New Zealand White Rabbit: A Novel Model for Prolapse Mesh Implantation via a Lumbar Colpopexy. *International Urogynecology Journal* 2019 (Accepted, article in press and yes acknowledgement of federal support was made)

Books or other non-periodical, one-time publications: Nothing to Report

Other publications, conference papers, and presentations:

*Knight K.M., Moalli P.A., Abramowitch S.D. Preventing Mesh Pore Collapse Through Auxetic Geometries: A Comprehensive Evaluation via Computational Modeling. American Urogynecology Society 37th Annual Scientific Meeting, Denver, CO, September 27 – October 1, 2016

Knight K., Abramowitch S., Moalli P. In vivo Evaluation of the Host Response to an Elastomeric Mesh: An Alternative to Polypropylene Mesh. American Urogynecology Society 38th Annual Scientific Meeting, Providence, Rhode Island, October 3-7, 2017

*Knight KM., King GE., Palcsey SL., Moalli PA., Abramowitch SD. Impact of Prolapse Mesh on Vaginal Smooth Muscle Function: A Comparison Between the Rabbit and Nonhuman Primate. Society for Pelvic Research, Reno, Nevada, December 2-3, 2017

Knight KM, Moalli PA, Abramowitch SD. Development and Evaluation of an Elastomeric Mesh for Pelvic Organ Prolapse Repair: An Alternative to Knitted, Polypropylene Mesh. 8th World Congress of Biomechanics, Dublin, Ireland, July 8-12, 2018

Knight K, Abramowitch S, Moalli P. *In vivo* Evaluation of the Host Response to an Elastomeric Mesh: An Alternative to Polypropylene Mesh. Magee-Womens Research 9-90 Summit, Pittsburgh, PA, October 9-10, 2018

*Knight KM, Artsen AM, King GE, Palcsey SL, Abramowitch SD, Moalli PA. The New Zealand White Rabbit: An Alternative Model for Studying the Impact of Polypropylene Mesh on Vaginal Smooth Muscle Morphology and Function. American Urogynecology Society 39th Annual Scientific Meeting, Chicago, Illinois, October 9-13, 2018

Iftikhar, A. Nolfi AL, Artsen AM, Moalli PA. A Clinically Relevant Rabbit Surgical Model of Pelvic Reconstruction to Evaluate the Immune Response to Mesh in the Abdomen and Vagina. American Urogynecology Society 39th Annual Scientific Meeting, Chicago, Illinois, October 9-13, 2018

Knight K.M., Artsen A.M., King G.E., Palcsey S.L., Abramowitch S.D., Moalli P.A. Stiff vs Soft – Exploring the Role of Material Stiffness on Vaginal Contractile Function and Composition. American Urogynecology Society/International Urogynecological Association Joint Scientific Meeting, Nashville, Tennessee, September 24-28, 2019

Website(s) or other Internet site(s):
Our organization has updated the Magee-Womens Research Institute Website which details our research projects and publications. https://mageewomens.org/investigator/pamela-moalli-md-phd/

Technologies or techniques: Nothing to Report

Inventions, patent applications, and/or licenses:

The University of Pittsburgh has released the technology to us and we have received a letter from the U.S. Army Medical Research and Development Command stating that the Army releases the technology to us as well. We are currently in the process of completing the final paperwork to have the Army official release the technology to us at which point we will pursue a patent application with another entity.

Other Products: Nothing to Report

7. PARTICIPANTS & OTHER COLLABORATING ORGANIZATIONS

What individuals have worked on the project?

Name:	Pamela Moalli, Principal Investigator
Nearest person month worked:	0.8
Contribution to Project:	She oversaw the biochemical, histomorphology and immunofluorescence outcomes. She held weekly lab meetings with all of the personnel and staff included in this grant, reviewed all technical aspects of data procurement, data obtained from the experiments, data analysis, and manuscript preparation.
Name:	Rui Liang, Research Associate
Nearest person month worked:	0.85
Contribution to Project:	Dr. Liang was in charge of overseeing day to day activities regarding the biochemical, histomorphology and immunofluoresence outcomes.

Has there been a change in the active other support of the PD/PI(s) or senior/key personnel since the last reporting period? No

What other organizations were involved as partners? Nothing to Report

8. SPECIAL REPORTING REQUIREMENTS

COLLABORATIVE AWARDS: N/A

QUAD CHARTS: N/A

9. APPENDICES:

1. Knight KM., Moalli PA., Abramowitch SD. Preventing Mesh Pore Collapse by Designing Mesh Pores with Auxetic Geometries: A Comprehensive Evaluation via Computational Modeling. *Journal of Biomechanical Engineering* 2018;140(5):051005-1-051005-8

2. Knight KM., Artsen AM., Routzong MR., King GE., Abramowitch SD., Moalli PA. New Zealand White Rabbit: A Novel Model for Prolapse Mesh Implantation via a Lumbar Colpopexy. *International Urogynecology Journal* 2019 (Accepted, article in press)

Preventing Mesh Pore Collapse by Designing Mesh Pores With Auxetic Geometries: A Comprehensive Evaluation Via Computational Modeling

Katrina M. Knight
Department of Bioengineering,
Musculoskeletal Research Center,
University of Pittsburgh,
405 Center for Bioengineering
300 Technology Drive,
Pittsburgh, PA 15219
e-mail: kmk144@pitt.edu

Pamela A. Moalli
Department of Obstetrics and Gynecology and
Reproductive Sciences,
Magee-Womens Research Institute,
Magee Womens Hospital,
University of Pittsburgh,
204 Craft Avenue,
Pittsburgh, PA 15213
e-mail: moalpa@mail.magee.edu

Steven D. Abramowitch[1]
Department of Bioengineering,
Musculoskeletal Research Center,
University of Pittsburgh,
Magee-Womens Research Institute,
Magee-Womens Hospital,
University of Pittsburgh,
309 Center for Bioengineering
300 Technology Drive,
Pittsburgh, PA 15219
e-mail: sdast9@pitt.edu

Pelvic organ prolapse (POP) meshes are exposed to predominately tensile loading conditions in vivo that can lead to pore collapse by 70–90%, decreasing overall porosity and providing a plausible mechanism for the contraction/shrinkage of mesh observed following implantation. To prevent pore collapse, we proposed to design synthetic meshes with a macrostructure that results in auxetic behavior, the pores expand laterally, instead of contracting when loaded. Such behavior can be achieved with a range of auxetic structures/geometries. This study utilized finite element analysis (FEA) to assess the behavior of mesh models with eight auxetic pore geometries subjected to uniaxial loading to evaluate their potential to allow for pore expansion while simultaneously providing resistance to tensile loading. Overall, substituting auxetic geometries for standard pore geometries yielded more pore expansion, but often at the expense of increased model elongation, with two of the eight auxetics not able to maintain pore expansion at higher levels of tension. Meshes with stable pore geometries that remain open with loading will afford the ingrowth of host tissue into the pores and improved integration of the mesh. Given the demonstrated ability of auxetic geometries to allow for pore size maintenance (and pore expansion), auxetically designed meshes have the potential to significantly impact surgical outcomes and decrease the likelihood of major mesh-related complications.
[DOI: 10.1115/1.4039058]

Keywords: bowtie mesh, pelvic organ prolapse, Poisson's ratio, polypropylene, uniaxial/tensile loading

1 Introduction

Synthetic meshes are commonly used in the repair of pelvic organ prolapse (POP), one of the most prevalent pelvic floor disorders characterized by the descent of the pelvic organs into the vaginal canal. Of the 300,000 surgeries performed to repair POP in 2010, one-third involved the use of mesh. In spite of a good anatomic success rate of approximately 82%, mesh usage has been hampered by complications with mesh exposure through the vaginal epithelium and pain being the two most commonly reported [1,2]. Recent research suggests that collapse of the mesh pores may be contributing to the pathogenesis of POP mesh complications [3,4].

The majority of current POP meshes are simply hernia meshes remarketed for POP repair. Additionally, these devices are manufactured from polypropylene and typically have large pores (i.e., >1 mm) with a porosity (defined as the amount of void space in a mesh relative to the mesh area) that is greater than 55%. However, these characteristics describe the mesh in the unloaded state and prior to implantation. In vivo, the dominating forces applied to POP meshes are tensile [3]. Unlike hernia meshes, in which tension is applied circumferentially, tension in POP mesh applications primarily occurs unidirectionally either along the longitudinal axis of the mesh (sacrocolpopexy) or along mesh arms (transvaginal mesh procedures). Meshes that are not constrained or tensioned uniformly around their perimeter change shape, and this change largely results from a reorientation and modification in the structural geometry of the mesh pores [5,6]. In many cases, the application of tension well within the physiologic range causes the pores of most POP meshes to collapse, resulting in pore diameters that are less than 1 mm—a critical size for tissue ingrowth [3,7].

Meshes with small pores and low porosity are associated with increased inflammation and fibrosis and yield poor tissue integration with decreased collagen deposition relative to meshes with large pores and high porosity [8–11]. Additionally, smaller pores increase the risk of bridging fibrosis (overlapping of the foreign body response to neighboring fibers), a process that can lead to encapsulation and pain [10,11]. Clinically, mesh contraction (i.e., pores collapsing) is associated with vaginal pain, and interestingly, problematic areas for patients experiencing mesh complications are often located in areas where the pores of a mesh have collapsed after tensioning and/or loading [4]. Collectively, these findings strongly suggest that controlling the response of pores to loading is a critical design consideration in the development of POP meshes that has the potential to lead to better host integration and fewer complications.

With a long-term goal of overcoming the problem of pore collapse and mesh contraction, we proposed to design synthetic meshes with auxetic pore geometries. The term auxetic refers to materials that have a negative Poisson's ratio and structures that demonstrate behaviors such as lateral expansion when placed in tension. This type of behavior is counterintuitive given that most materials contract or narrow in the transverse direction when stretched longitudinally, i.e., they have a positive Poisson's ratio. To date, auxetic geometries have been utilized to manufacture annuloplasty prostheses for cardiac valve repair surgery, artificial intervertebral disks, cushion pads, and knee prosthetics [12,13].

[1]Corresponding author.
Manuscript received August 22, 2017; final manuscript received January 8, 2018; published online March 1, 2018. Assoc. Editor: Jeffrey Ruberti.

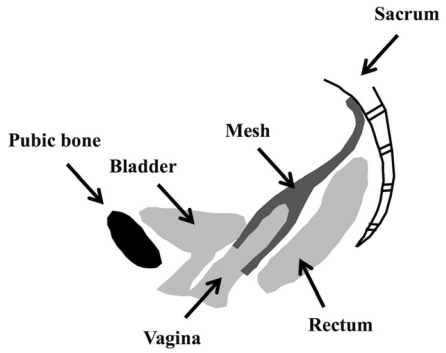

Fig. 1 Schematic of a sacrocolpopexy in which the mesh is attached to the anterior and posterior walls of the vagina and fixed to the sacrum. In vivo intra-abdominal pressure exerts a downward force on the pelvic organs. This results in a tensile force along the longitudinal axis of the mesh.

However, beyond these applications, there has been limited use of auxetic geometries within the biomedical field. The development of a mesh with pores designed to open in response to tension as opposed to contracting has the potential to be highly beneficial in regards to the development of meshes for POP repair.

The objective of this study was to assess the behavior of auxetic pore geometries with tensile loading and to evaluate their potential to provide resistance to tensile loads while simultaneously undergoing pore expansion. To minimize cost, time, and the introduction of additional variables resulting from manufacturing and mechanical testing of each design, this investigation utilized a standard engineering workflow whereby finite element analysis (FEA) was used to provide an objective first investigation to identify auxetic geometries that should be explored further as potential pore designs for POP meshes intended for sacrocolpopexy. Tension is primarily applied along the longitudinal axis of the mesh when implanted via a sacrocolpopexy (Fig. 1). The purpose of the mesh in a sacrocolpopexy is to reinforce the vaginal walls, stabilize the apex (superior) of the vagina, and to resist the motion of the distal vagina resulting from an increase in abdominal pressure. From a gross mechanical perspective, mesh function for a sacrocolpopexy is in many ways analogous to a tether. Thus, eight computational models of meshes with auxetic pore geometries (referred to as auxetic models) were constructed and subjected to simulated uniaxial tensile tests via three-dimensional quasi-static, large deformation finite element analysis. For comparison, computational models of meshes with standard pore geometries (i.e., pore shapes that are commonly used for commercial synthetic meshes) were also created and exposed to the same simulated boundary conditions as the computational models with auxetic pores. These models are referred to as standard models. Quantitative measurements of the minimal pore diameter, porosity, effective porosity, effective pore area, and overall expansion (or contraction) of the models' width, via calculation of the relative lateral contraction, were used to characterize the deformation of the pore geometries and models overall.

2 Materials and Methods

2.1 Design of Models Using Computer-Aided Design. Eight models with auxetic pore geometries and three models with standard pore geometries were generated using the computer-aided design (CAD) software, SOLIDWORKS 2013 ×64 Edition (Dassault Systèmes SOLIDWORKS Corporation, Waltham, MA). The pore geometries for the auxetic models included (1) bowtie (B), (2) spiral (S), (3) triangle (T), (4) square chiral(a) (SCa), (5) chiral hexagon (CH), (6) square chiral(b) (SCb), (7) hexagon(b) (Hb), and (8) square grid (SG) (Fig. 2). These geometries were chosen as they were deemed to be without obvious limitations that would

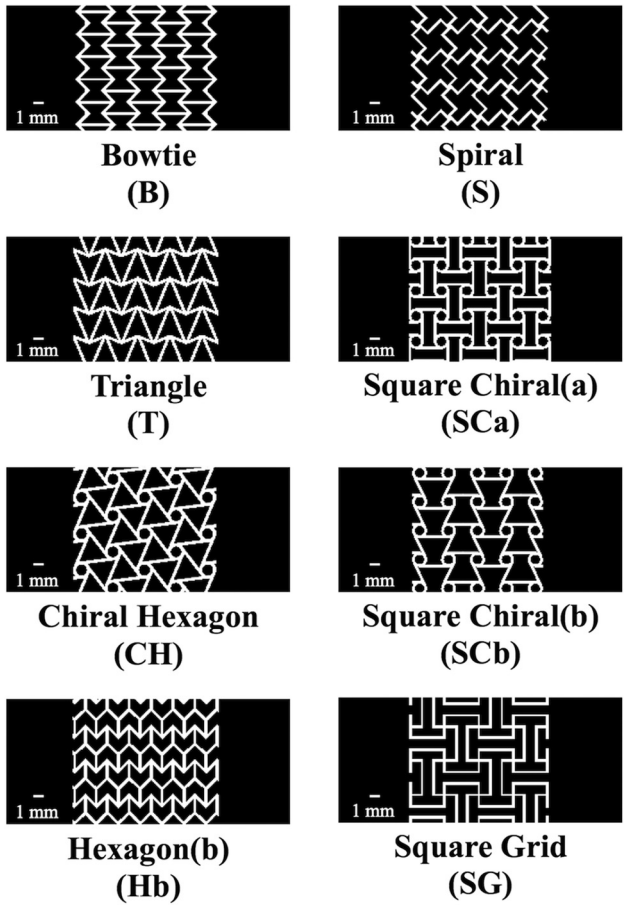

Fig. 2 Orthographic frontal plain views of three-dimensional auxetic CAD models with eight different auxetic pore geometries. Note the models pictured represent only a portion of the total length of the CAD models utilized in the FEA.

negatively impact performance or manufacturability by authors of this paper with significant mesh expertise (Pamela Moalli and Steven Abramowitch).

Currently, the majority of commercially available POP meshes have pores that are either square, diamond, or hexagon shaped; therefore, these three shapes were used to construct the standard CAD models in this study. Specifically, the standard CAD models with square- and diamond-shaped pores were simplified geometries modeled after Restorelle (Coloplast, Minneapolis, MN) POP mesh, and the CAD model with hexagon-shaped pores was a simplified geometry modeled after Gynemesh PS (Ethicon, Somerville, NJ) POP mesh. Calipers were used to measure the fiber width (distance between two fibers), thickness, and the pore size of the commercial products. These dimensions were ultimately used to guide the development of the standard models which included (1) square (SQ), (2) diamond (D), and (3) hexagon(a) (Ha) (Fig. 3).

Additionally, to create a realistic model with auxetic pore geometries, the dimensions (i.e., fiber width, thickness, and pore size) of the auxetic model pores were also modeled after Restorelle. The latter was chosen as the "model mesh" given the relative simplicity of the pore geometry (square pore geometry) and the ease of measuring the dimensions of these pores. However, it is important to note that the pore size of the auxetic pore geometries did not exactly match those of Restorelle due to the design/complexity of these geometries.

The pores of each model were designed with specific considerations. First, the width of the fibers equaled 0.30 mm, and the minimal pore diameter was at least 1 mm. The latter was the maximum pore size that could be achieved given the fiber width, geometry of the pore, and the requirement that the volume of material was

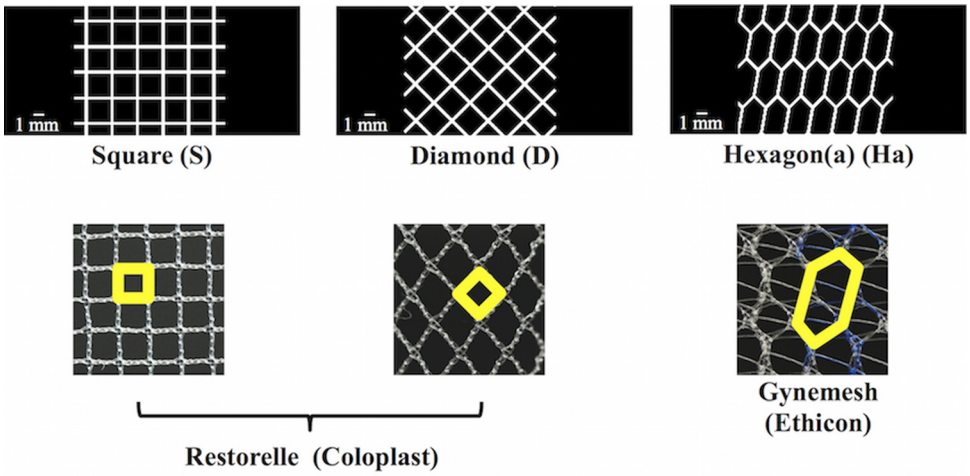

Fig. 3 Standard CAD models (top images) were created with square, diamond, and hexagon shaped pores, which are commonly used pore shapes for commercial synthetic meshes (bottom images). Note, the outlined shapes (in bold) in the commercial images represent the geometry that was used to create the respective CAD model. Actual images of mesh (bottom images) are 10 mm × 10 mm.

consistent from model to model. Indeed, the majority of the models had pore dimensions that were greater than 1 mm. It should also be noted that models containing angles less than 90 deg would have small regions of the pore where two fibers would be closer than 1 mm (i.e., intersections of model fibers forming corners). To balance our interest in maximizing these spaces without compromising the auxetic behavior of any specific geometry, the smallest allowable angle within a pore was restricted to 45 deg. For designs containing circles, the diameter of the circles was equal to 1 mm.

All models had an overall length of 84.75±4.80 mm and average width of 14.79±0.82 mm resulting in an aspect ratio of at least 5. Additionally, the average volume of all models was 91.54±0.66 mm^3. There was a slight variation between designs on these values, because the shape of individual pores would create inconsistencies when boundary conditions were applied to the model that would result in numerical instabilities in the simulations and biased comparisons between models. Thus, we aimed to keep these values as close as possible between designs.

2.2 Computational Analysis. Standard and auxetic CAD models were discretized and refined using Autodesk Simulation Mechanical (Autodesk, Inc., San Rafael, CA) and Gmsh (V2.11.0), respectively. Discretized finite element models consisted of a combination of tetrahedral, pentahedral, and hexahedral elements ranging from 178,944 to 705,088 total elements per model. The Neo-Hookean material was defined for all models. Although the actual magnitude of the elongations achieved for an applied force was not as relevant as the relative elongations between mesh designs in this study, we nevertheless wanted to choose material parameters that resulted in elongations that were consistent with current mesh products. Thus, the material parameters used for all models were obtained via an inverse optimization analysis in which the uniaxial load-elongation data of Restorelle was fit to a computational simulation of Restorelle, which had the same dimensions as the physical mesh tested. Based on this optimization, it was determined that the Neo-Hookean material with a Young's Modulus of 52.98 MPa and Poisson's ratio of 0.41 could accurately describe the nonlinear load-elongation behavior of Restorelle (Fig. 4). Thus, these material parameters were utilized for all models.

Simulated uniaxial tensile tests were performed using FEBio Software Suite (University of Utah, MRL). Specifically, a rigid body was fixed to the top edge of each model allowing the rigid body to drive the displacement (Fig. 5). The rigid body was only allowed to move vertically. This allowed for the top edge of each

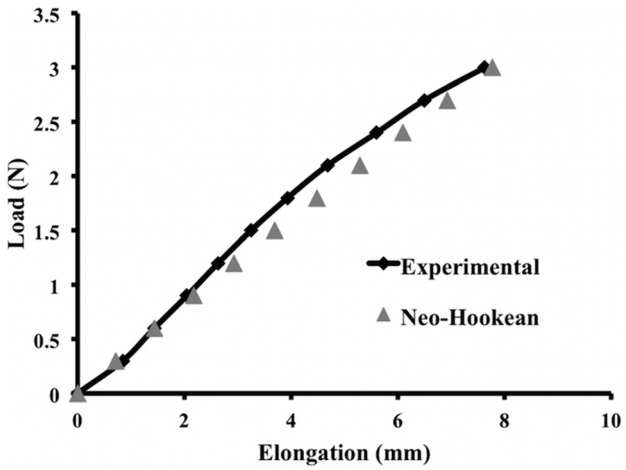

Fig. 4 Finite element simulation of the square pore model with a Neo-Hookean material (Neo-Hookean, triangle) was able to accurately capture the ex vivo, nonlinear load-elongation behavior of Restorelle uniaxially loaded to 3 N (experimental, diamond)

model to be limited to only vertical displacement resulting from the application of a 3 N vertical load to the rigid body. The bottom edge of each model was fixed in translation and rotation. All deformation was constrained to be in the frontal plane of the model. The resulting deformed solution for all discretized models was obtained and postprocessed to quantify the following parameters: relative elongation, minimal pore diameter, effective pore area (area of the pores with diameters that are greater than 1 mm) [14], porosity, effective porosity (percent of void space from pores with minimal diameters that are greater than 1 mm) [14], and relative lateral contraction (analogous to the Poisson's ratio for a continuous material). Three Newtons represents the minimal amount of force that a mesh must be able to withstand based on our estimates of the surface area of the anterior vagina using magnetic resonance imaging measurements and estimates of the intra-abdominal pressure reported with sitting and standing [15–19].

2.3 Quantification of Parameters. Relative elongation was calculated by dividing the amount that the model elongated in response to 3 N by the initial length of the model. To quantify the

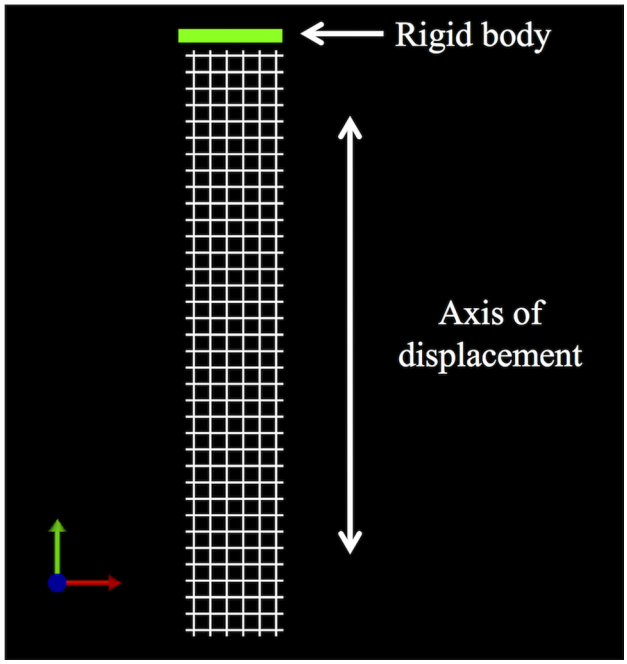

Fig. 5 To simulate a uniaxial tensile test, the bottom edge of the models was fixed in translation and rotation, while the top edge was fixed to a rigid body

minimal pore width, effective pore area, porosity, and effective porosity, a custom Mathematica V10 (Wolfram, Champaign, IL) script was utilized. These parameters were calculated for the pores within a 30 mm × 12 mm section of the mid-region of the models. The previously mentioned dimensions were chosen as they captured the repeating geometry of the pores. Additionally, focusing on those pores within the midregion of the model minimized the influence of edge effects on pore deformation. A similar method was used by Barone et al. [3]. Briefly, screenshots of the midregion of the models in the undeformed (0 N) and deformed (3 N) states were taken and imported into Mathematica. Images were then binarized and an edge detection algorithm was used to identify the fibers of the model (black pixels) and the pores (white pixels). Unlike the previous parameters, the relative lateral contraction was calculated for the models using images of the entire model (i.e., lateral edge to lateral edge). The undeformed (0 N) and deformed model images (assessed at loads of 0.6 N, 1.5 N, 2.4 N, and 3 N) were imported into a custom MATHEMATICA V10 (Wolfram, Champaign, IL) script, and the pores were identified using algorithms as described previously. Next, the center of mass (i.e., the centroid) was located for each pore, and the coordinate position of these centroids, in the un-deformed and deformed states, was exported. These positions were then used to calculate the relative lateral contraction as follows: relative lateral contraction $= -(\text{relative elongation}_{\text{transverse}}/\text{relative elongation}_{\text{longitudinal}})$. This parameter is representative of the degree of contraction with a positive value indicating contraction (i.e., pore collapse—typical of most materials and structures) and a negative value indicating expansion (i.e., pores remaining open/enlarging), consistent with the definition of Poisson's ratio for continuous materials.

2.4 Model Assessment Criteria. The following four criteria were used to define what would be clinically considered to be a positive mesh response to uniaxial loading in vivo.

(1) The pores can expand but the overall geometry of the pore should not be dramatically reoriented (e.g., a significant degree of rotation) in response to loading. It is believed that significant motion between the mesh and the host can negatively impact the host response to an implant, and this phenomenon has been demonstrated for percutaneous implants at the skin–device interface and for dental implants at the implant–bone interface [20,21].
(2) The minimal pore diameter should be at least 1 mm, and the effective pore area as well as the porosity and effective porosity should be maintained following the application of load. In both the abdominal hernia and urogynecology literature, large pore, high porosity meshes yield better tissue integration with increased collagen deposition between the pores and decreased inflammation and fibrosis relative to meshes with small pores and low porosity [8–11]. For polypropylene meshes, 1 mm is identified as the optimal minimal pore diameter needed to allow for tissue ingrowth and to prevent bridging fibrosis [10].
(3) A negative relative lateral contraction will signify mesh expansion, which is considered to be a beneficial response to loading for POP meshes. Contraction of POP meshes is associated clinically with vaginal pain, dyspareunia (pain with sexual intercourse), and tenderness upon palpation of the contracted portion of the mesh [4]. Additionally, when pores contract, the chances of bridging fibrosis increases [11]. It is therefore important that the mesh width overall, and hence the pores, are maintained or expand with loading.
(4) Overall the amount of mesh elongation should be minimal to provide maximal stiffness of the mesh (i.e., reduce the risk of recurrence) with a minimal amount of material. In other words, the mesh should be as stiff as possible using the least amount of material. This is complicated by the fact that the structural stiffness of the overall mesh results from the interconnections and orientations of fibers that provide specific pore geometries, the stiffness of the material that composes those fibers (e.g., polypropylene), and the amount of that material (heavy versus light weight). Clinically, lightweight meshes have been shown to be more favorable relative to heavyweight meshes [10,22–25]. Thus, if a mesh design undergoes greater elongation relative to another design, more material (heavier weight) would be required to make them equal. Alternatively, a stiffer material could also be substituted, potentially at the risk of causing a significant stiffness mismatch between the mesh and the vagina. In this study, both the amount of material and stiffness of the material were held consistent between models so that the impact of pore geometry on relative elongation of the mesh could be assessed. This was accomplished by assigning the same constitutive model and same model parameters for each simulation and ensuring that the dimensions and volume of material used for each model was consistent across all model designs.

3 Results

3.1 Convergence Testing. Using the boundary conditions described previously, model convergence (specifically convergence of model elongation, minimal pore diameter, and pore length) was performed for all 11 model designs using the h-refinement method. Models were considered to achieve convergence when an increase in the number of elements resulted in a less than 5% difference in the three parameters. In this study, three to four levels of refinement were utilized using a combination of tetrahedral, pentahedral, and hexahedral elements ranging from a total of 178,944 to 705,088 elements across model designs (Table 1). The results reported are for simulations in which the model elongation, minimal pore diameter, and pore length all converged within 5%. See Supplemental Figs. 1–3 for graphs of the convergence results, which are available under "Supplemental Data" tab for this paper on the ASME Digital Collection.

3.2 Computational Results. The pore and overall model deformation of the CAD models with three standard and eight

Table 1 Composition of finite element models in terms of element. Numbers represent the amount of elements in each category listed in the heading.

	Tetrahedral elements	Pentahedral elements	Hexahedral elements	Total number of elements
Square	0	0	178,944	178,944
Diamond	0	0	228,480	228,480
Hexagon(a)	21,056	39,744	199,616	260,416
Bowtie	258,432	181,184	265,472	705,088
Spiral	0	0	224,768	224,768
Triangle	218,240	105,152	300,224	623,616
Square chiral(a)	212,800	177024	286,656	676,480
Chiral hexagon	167,296	204,352	242,944	614,592
Square chiral(b)	63,680	74,752	206,656	345,088
Hexagon(b)	162,432	167,872	314,880	645,184
Square grid	20,800	17,472	325,376	363,648

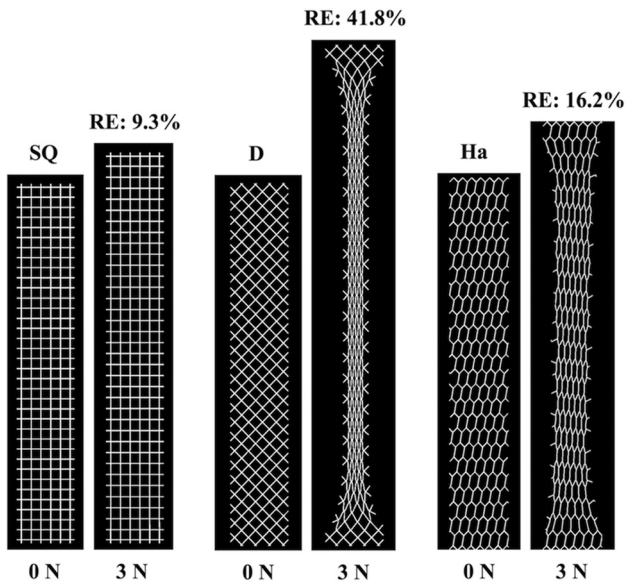

Fig. 6 FEA results at 0 N and 3 N for the standard models. The pores of the square model (SQ) remained relatively open, whereas the pores of the diamond (D) and hexagon(a) (Ha) models collapsed resulting in model contraction. RE = relative elongation.

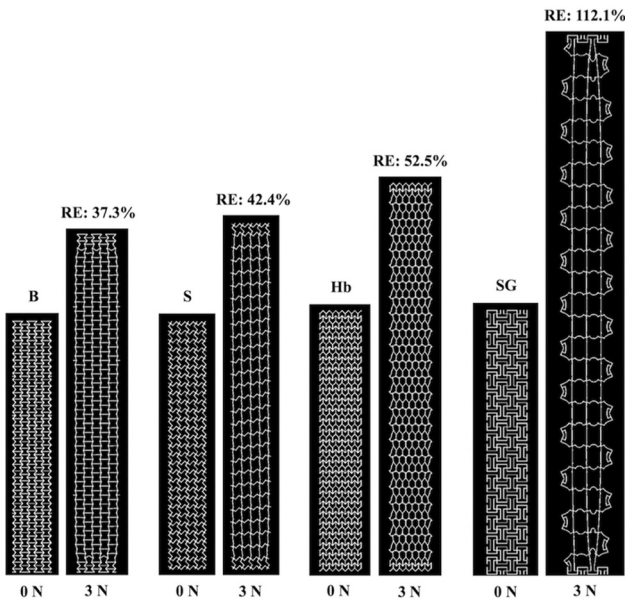

Fig. 7 FEA results at 0 N and 3 N for the bowtie (B), spiral (S), hexagon(b) (Hb), and square grid (SG) auxetic models. Pore expansion is apparent for all models pictured. RE = relative elongation.

auxetic pores in response to 3 N of force was assessed via simulated uniaxial tensile tests. For the standard models, only the pores of the square model remained opened, whereas the pores of the diamond and hexagon(a) models contracted (Fig. 6). For the auxetic models, pore expansion was visibly apparent for four of the eight models: the bowtie, spiral, hexagon(b), and square grid models (Fig. 7). The triangles and the circles within the remaining four auxetic models (triangle, chiral hexagon, square chiral(a), and square chiral(b)), all contracted (Fig. 8). Overall, the pores of the square grid model experienced the most dramatic change in pore shape, changing from an initial collection of rectangles to large squares (Fig. 7). Upon qualitative assessment of the models, expansion of the bowtie, square chiral(a), and square grid models was visibly apparent unlike the diamond and hexagon(a) models, which contracted. The subtle changes in the deformation of all other models made it difficult to qualitatively determine whether these models expanded or contracted in response to 3 N. However, assessing the overall elongation of each model, it was clear that the pore geometry impacted how much the model elongated. Specifically, the square and hexagon(a) models deformed the least with relative elongations of 9.3% and 16.2%, respectively, while the square grid model deformed the most, elongating 112.1% more than its initial length.

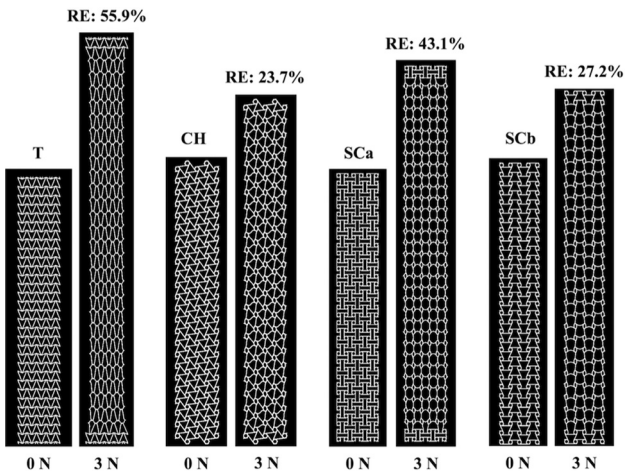

Fig. 8 FEA results at 0 N and 3 N for the triangle (T), chiral hexagon (CH), square chiral(a) (SCa), and square chiral(b) (SCb) auxetic models. The triangles and circles within these models all contracted. RE = relative elongation.

Table 2 Characterization of pore deformation via quantification of the percent change in minimal pore diameter, effective pore area, porosity, and effective porosity

CAD model	Minimal pore diameter % change	Effective pore area % change	Porosity % change	Effective porosity % change
Square	−3.9%	No change[a]	+2.7%	+2.7%
Diamond	−81.6%	−100%	−33.3%	−100.0%
Hexagon(a)	−43.5%	No change[a]	−12.5%	−12.5%
Bowtie	+113.0%	No change[a]	+25.9%	+25.9%
Spiral	−2.0%	No change[a]	+12.9%	+12.9%
Triangle	−30.2%	No change[a]	+14.5%	+14.5%
Square chiral(a)	−32.0%	−13.0%	+15.0%	No change[b]
Chiral hexagon	−18.9%	−10.7%	+6.9%	−5.2%
Square chiral(b)	−32.7%	−12.3%	+15.3%	No change[b]
Hexagon(b)	+125.0%	No change[a]	+21.4%	+21.4%
Square grid	+443.0%	No change[a]	+40.3%	+40.3%

[a]Initially, the effective pore area for all CAD models was 100%; thus, no change means that the effective pore area at 3 N was maintained at 100%.
[b]No change—the effective porosity before (0 N) and after loading (3 N) are the same.

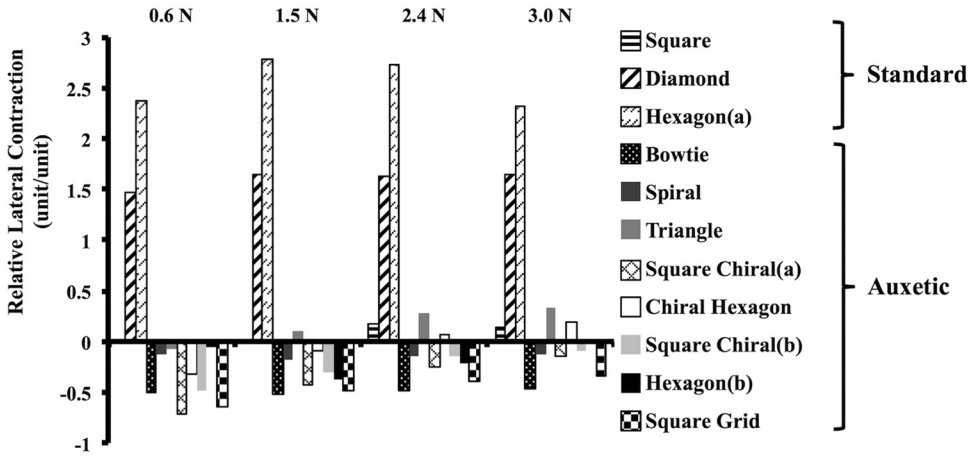

Fig. 9 Relative lateral contraction results with increasing tension for both the standard and auxetic models. As anticipated, the relative lateral contraction was positive for the nonauxetic models for all levels of tension. Initially, the relative lateral contraction was negative for all auxetic models. However, at 1.5 N and 2.4 N, the relative lateral contraction was positive (and remained positive) for the triangle and chiral hexagon models, respectively. A positive value indicates model contraction, and a negative value indicates expansion.

Quantitatively assessing the deformation of the pores at 3 N, the minimal pore diameter of the diamond, square chiral(a), chiral hexagon, and square chiral(b) models decreased below 1 mm (see Supplemental Fig. 4, which is available under "Supplemental Data" tab for this paper on the ASME Digital Collection). The observed decrease in the minimal pore diameter also translated to a complete loss or decrease in the effective pore area for the previously mentioned models. The effective pore area was maintained at 100% for all other models (square, hexagon(a), bowtie, spiral, triangle, hexagon(b), and square grid). In addition to the effective pore area, the deformation of the pores was characterized via quantification of the porosity and effective porosity. In response to 3 N of force, the porosity decreased for the diamond and hexagon(a) models, while the porosity of the square model and all auxetic models increased. A decrease in the effective porosity was observed for the diamond, hexagon(a), and chiral hexagon models, whereas the effective porosity remained the same or increased for all other models in response to 3 N. See Table 2 for a summary of these results.

Interesting results were observed when assessing the expansion of the models via quantification of the relative lateral contraction (Fig. 9). The relative lateral contraction for the standard pore models was positive, signifying lateral contraction of these models, and this result was expected given that the pores of these models were nonauxetic. Consistent with auxetic behavior, the relative lateral contraction for all models with auxetic pores was negative at lower loads indicating lateral expansion. However, at 1.5 N and 2.4 N, the relative lateral contraction was positive and remained positive with additional loading for the triangle and chiral hexagon models, respectively. For all other models (the bowtie, spiral, square chiral(a), square chiral(b), hexagon(b), and square grid) the relative lateral contraction remained negative throughout loading signifying lateral expansion with the bowtie expanding the most.

4 Discussion

In this study, the behavior (i.e., pore deformation and the overall expansion or contraction) of synthetic mesh models with auxetic pore geometries in response to 3 N of uniaxial tension was assessed using computational modeling. For comparison, the behavior of models with standard pore geometries was also analyzed. Congruent with our hypothesis, models with auxetic pore geometries designed to expand in response to uniaxial loading did not experience pore collapse with loading. However, one important caveat to note is that using auxetic shapes as pore geometries does not guarantee that the pores will remain open and that the model as a whole will expand indefinitely. For example, the triangle and chiral hexagon models both displayed contraction at 3 N despite initially expanding at lower tensions. This suggests that the auxetic behavior is not maintained for all auxetic geometries

with increasing tension. As anticipated, the models with standard pore geometries contracted and/or their pores collapsed with loading, and this result is consistent with ex vivo testing of commercial synthetic mesh products with similar pore geometries [3].

Given that the pores remained open for all models with auxetic pore geometries, the question of which auxetic geometry is best for POP repair arises. This study only investigated mesh geometries and loading conditions that are relevant to abdominal sacrocolpopexy. Based on the model assessment criteria outlined in Sec. 2.4, the square grid geometry is not appropriate for abdominal sacrocolpopexy given that the square grid pores rotated which resulted in significant pore deformation. This pore rotation allowed the square grid model to elongate more than any other model (more than doubling in length), which would necessitate the use of more material or a stiffer material to achieve the smaller deformed lengths observed in the other models. The auxetic geometries with circles (chiral hexagon, square chiral(a), and square chiral(b)) demonstrated contraction of the circles with loading which resulted in a minimal pore diameter that was less than 1 mm, ultimately decreasing the effective porosity. Meshes with pores less than 1 mm can become encapsulated due to bridging fibrosis—a phenomenon that has been associated with pain [26]. One way to overcome this limitation is to increase the diameter of the circles. However, this change would likely negatively impact the elongation of these designs, because there would be less material to resist the same amount of tension; thus, the chiral hexagon, square chiral(a), and square chiral(b) were determined to be inferior by our criteria.

Of the remaining four auxetic geometries (bowtie, spiral, triangle, and hexagon(b)), the relative lateral contraction of the triangle model was positive at 3 N, and therefore, the triangle auxetic geometry was excluded. The bowtie stood out as the most favorable geometry due to its increasing porosity and greater effective porosity with loading. The bowtie model also deformed the least and had the greatest increase in porosity and effective porosity compared to the spiral and hexagon(b) models. Additionally, relative to all other models, the relative lateral contraction was the most negative for the bowtie model. Given these promising results, the bowtie geometry shows significant potential and likely warrants focus of additional investigations. However, it is important to note that these qualities arise at the expense of increased elongation relative to the square pore standard geometry. Additionally, the uniaxial response to 3 N of tension for the bowtie model, and all other models simulated in this study, is specific to the direction in which it was loaded and to the amount of tension applied. Although not explored in this study, a rotation of the bowtie geometry by 45 deg with respect to the loading axis would likely result in destabilization of the pore with pore collapse and a decrease in the effective porosity. Similarly, increasing the amount of tension applied to the bowtie model (and all other auxetic models that experienced pore expansion) would likely alter the pore deformation and could possibly result in pores contracting and/or collapsing. Thus, the bowtie geometry may only be suited for sacrocolpopexy repairs within a certain range of tension.

Comparison of the behavior of the standard pore models, particularly the square pore model, to the auxetic models demonstrated the strengths of the auxetic pore geometry. Arguably, the square pore geometry performed just as well as the bowtie. In response to the applied load of 3 N, the pores of the square model remained open and the minimal pore diameter was greater than 1 mm. Additionally, the square model deformed the least overall, the effective pore area was maintained at 100%, and the porosity and effective porosity both increased for this model. However, the relative lateral contraction of the square model was positive, implying that the model contracted. In addition to the model contracting, the individual pores also contracted (from an average minimal diameter of 2.04 mm to 1.96 mm). Although minimal, it is important to note that this small amount of contraction is in response to a very low load (3 N), and we are utilizing an idealized geometry that does not account for the influence of the mesh knit pattern. In vivo, intra-abdominal forces are higher than 3 N with activities such as jumping, coughing, and sneezing. Additionally, the knit pattern can also contribute to changes in pore geometry with increasing tension that were not predicted in this study. With those caveats, it is nevertheless interesting that in vivo implantation studies by Feola et al. and Liang et al. showed that a square pore mesh performs better in terms of its impact on vaginal smooth muscle function and morphology as well as collagen and elastin content compared to other POP meshes with pore geometries that are more likely to collapse in response to tension [27,28]. These findings are congruent with what would be predicted based on the results of this study. However, it is also important to understand that other factors including the structural stiffness and weight of each mesh may have also contributed to those in vivo findings [10,22–25,27–31].

The way in which the auxetic and standard models were designed and evaluated is a major strength of this study. The aspect ratio (length to width), fiber width, and the amount of material (the volume) were consistent for all models. Other constraints on angulation and pore diameters allowed us to focus on specific designs based on clinical relevance. Additionally, this allowed for a reduction of the possible solution space for auxetic designs and a comparison between designs that minimized bias. By designing this study in this way, the impact of the pore geometry on the overall behavior of the model could be evaluated and compared as the dependent variable. Changing these parameters (e.g., increasing and decreasing angles, thickness, stiffness, etc.) will likely produce numerical values that are different from the ones reported in this study.

In addition, the utilization of FEA allowed for us to establish reasonable first approximations of mesh behavior with auxetic pores without the cost, time, and introduction of variables related to manufacturing and experimental testing if these tests were to have been performed on physical samples. However, FEA is also limiting in that the results obtained are theoretical predictions and must be validated. Thus, future studies will aim to manufacture and mechanically test the most promising model designs identified in this study.

As a final note, the term "mesh" is typically used to describe a textile that is knitted or woven. The models evaluated in this study are more appropriately described as mesh analogues since behaviors of knots and other factors (knit/weave patterns, etc.) were not simulated.

Overall, this work provides an initial proof of concept that constructing meshes with auxetic pore geometries can prevent pore collapse and mesh contraction. Based on the previous research highlighting the importance of pore size, this novel mesh design is likely to afford better ingrowth of host tissue into the pores, host integration of the mesh, and also decrease the likelihood of bridging fibrosis. Successfully designing an auxetic mesh, as described, may significantly reduce the occurrence of major mesh-related complications.

Funding Data

- National Science Foundation Graduate Research Fellowship Program (Grant No. DGE-1247842).
- Office of the Assistance Secretary of Defense for Health Affairs, through Peer Reviewed Medical Research Program, U.S. Department of Defense (Grant No. W81XWH-16-1-0133).

References

[1] U.S. Food and Drug Administration, 2011, "Surgical Mesh for Treatment of Women With Pelvic Organ Prolapse and Stress Urinary Incontinence—FDA Executive Summary," U.S. Food and Drug Administration, Silver Spring, MD, accessed Jan. 29, 2018, http://www.thesenatorsfirm.com/documents/OBS.pdf

[2] Altman, D., Väyrynen, T., Engh, M. E., Axelsen, S., and Falconer, C., 2011, "Anterior Colporrhaphy Versus Transvaginal Mesh for Pelvic-Organ Prolapse," New Engl. J. Med., **364**(19), pp. 1826–1836.

[3] Barone, W. R., Moalli, P. A., and Abramowitch, S. D., 2016, "Textile Properties of Synthetic Prolapse Mesh in Response to Uniaxial Loading," Am. J. Obstet. Gynecol., **215**(3), p. 326.
[4] Feiner, B., and Maher, C., 2010, "Vaginal Mesh Contraction: Definition, Clinical Presentation, and Management," Obstet. Gynecol., **115**(2), pp. 325–330.
[5] Feola, A., Pal, S., Moalli, P., Maiti, S., and Abramowitch, S., 2014, "Varying Degrees of Nonlinear Mechanical Behavior Arising From Geometric Differences of Urogynecological Meshes," J. Biomech., **47**(11), pp. 2584–2589.
[6] Barone, W. R., Amini, R., Maiti, S., Moalli, P. A., and Abramowitch, S. D., 2015, "The Impact of Boundary Conditions on Surface Curvature of Polypropylene Mesh in Response to Uniaxial Loading," J. Biomech., **48**(9), pp. 1566–1574.
[7] Otto, J., Kaldenhoff, E., Kirschner-Hermanns, R., Mühl, T., and Klinge, U., 2014, "Elongation of Textile Pelvic Floor Implants Under Load Is Related to Complete Loss of Effective Porosity, Thereby Favoring Incorporation in Scar Plates," J. Biomed. Mater. Res. Part A, **102**(4), pp. 1079–1084.
[8] Greca, F. H., De Paula, J. B., Biondo-Simões, M. L. P., Da Costa, F. D., Da Silva, A. P. G., Time, S., and Mansur, A., 2001, "The Influence of Differing Pore Sizes on the Biocompatibility of Two Polypropylene Meshes in the Repair of Abdominal Defects: Experimental Study in Dogs," Hernia, **5**(2), pp. 59–64.
[9] Greca, F. H., Souza-Filho, Z. A., Giovanini, A., Rubin, M. R., Kuenzer, R. F., Reese, F. B., and Araujo, L. M., 2008, "The Influence of Porosity on the Integration Histology of Two Polypropylene Meshes for the Treatment of Abdominal Wall Defects in Dogs," Hernia, **12**(1), pp. 45–49.
[10] Klinge, U., Klosterhalfen, B., Birkenhauer, V., Junge, K., Conze, J., and Schumpelick, V., 2002, "Impact of Polymer Pore Size on the Interface Scar Formation in a Rat Model," J. Surg. Res., **103**(2), pp. 208–214.
[11] Orenstein, S. B., Saberski, E. R., Kreutzer, D. L., and Novitsky, Y. W., 2012, "Comparative Analysis of Histopathologic Effects of Synthetic Meshes Based on Material, Weight, and Pore Size in Mice," J. Surg. Res., **176**(2), pp. 423–429.
[12] Burriesci, G., and Bergamasco, G., 2007, "Annuloplasty Prosthesis With an Auxetic Structure," U.S. Patent No. US8034103 B2.
[13] Scarpa, F., 2008, "Auxetic Materials for Bioprostheses," IEEE Signal Process. Mag., **25**(5), pp. 126–128.
[14] Mühl, T., Binnebösel, M., Klinge, U., and Goedderz, T., 2008, "New Objective Measurement to Characterize the Porosity of Textile Implants," J. Biomed. Mater. Res. Part B Appl. Biomater., **84**(1), pp. 176–183.
[15] Cobb, W. S., Burns, J. M., Kercher, K. W., Matthews, B. D., James Norton, H., and Todd Heniford, B., 2005, "Normal Intraabdominal Pressure in Healthy Adults," J. Surg. Res., **129**(2), pp. 231–235.
[16] Howard, D., Miller, J. M., Delancey, J. O., and Ashton-Miller, J. A., 2000, "Differential Effects of Cough, Valsalva, and Continence Status on Vesical Neck Movement," Obstet. Gynecol., **95**(4), pp. 535–540.
[17] Hsu, Y., Chen, L., Tumbarello, J., Ashton-Miller, J. A., and DeLancey, J. O., 2010, "In Vivo Assessment of Anterior Compartment Compliance and Its Relation to Prolapse," Int. Urogynecol. J., **21**(9), pp. 1111–1115.
[18] Junginger, B., Baessler, K., Sapsford, R., and Hodges, P. W., 2010, "Effect of Abdominal and Pelvic Floor Tasks on Muscle Activity, Abdominal Pressure and Bladder Neck," Int. Urogynecol. J., **21**(1), pp. 69–77.
[19] Noakes, K. F., Pullan, A. J., Bissett, I. P., and Cheng, L. K., 2008, "Subject Specific Finite Elasticity Simulations of the Pelvic Floor," J. Biomech., **41**(14), pp. 3060–3065.
[20] Gao, S.-S., Zhang, Y.-R., Zhu, Z.-L., and Yu, H.-Y., 2012, "Micromotions and Combined Damages at the Dental Implant/Bone Interface," Int. J. Oral Sci., **4**(4), pp. 182–188.
[21] Holt, B., Tripathi, A., and Morgan, J., 2008, "Viscoelastic Response of Human Skin to Low Magnitude Physiologically Relevant Shear," J. Biomech., **41**(12), pp. 2689–2695.
[22] Klinge, U., Junge, K., Stumpf, M., Öttinger, A. P., and Klosterhalfen, B., 2002, "Functional and Morphological Evaluation of a Low-Weight, Monofilament Polypropylene Mesh for Hernia Repair," J. Biomed. Mater. Res., **63**(2), pp. 129–136.
[23] Klinge, U., Klosterhalfen, B., Conze, J., Limberg, W., Obolenski, B., Öttinger, A. P., and Schumpelick, V., 1998, "Modified Mesh for Hernia Repair That Is Adapted to the Physiology of the Abdominal Wall," Eur. J. Surg., **164**(12), pp. 951–960.
[24] Klinge, U., Klosterhalfen, B., Muller, M., Ottinger, A. P., and Schumpelick, V., 1998, "Shrinking of Polypropylene Mesh In Vivo: An Experimental Study in Dogs," Eur. J. Surg., **164**(12), pp. 965–969.
[25] O'Dwyer, P. J., Kingsnorth, A. N., Molloy, R. G., Small, P. K., Lammers, B., and Horeyseck, G., 2005, "Randomized Clinical Trial Assessing Impact of a Lightweight or Heavyweight Mesh on Chronic Pain After Inguinal Hernia Repair," Br. J. Surg., **92**(2), pp. 166–170.
[26] Nolfi, A. L., Brown, B. N., Liang, R., Palcsey, S. L., Bonidie, M. J., Abramowitch, S. D., and Moalli, P. A., 2016, "Host Response to Synthetic Mesh in Women With Mesh Complications," Am. J. Obstet. Gynecol., **215**(2), pp. 206.e1–206.e8.
[27] Feola, A., Abramowitch, S., Jallah, Z., Stein, S., Barone, W., Palcsey, S., and Moalli, P., 2013, "Deterioration in Biomechanical Properties of the Vagina Following Implantation of a High-Stiffness Prolapse Mesh," BJOG: Int. J. Obstet. Gynaecol., **120**(2), pp. 224–232.
[28] Liang, R., Abramowitch, S., Knight, K., Palcsey, S., Nolfi, A., Feola, A., Stein, S., and Moalli, P. A., 2013, "Vaginal Degeneration Following Implantation of Synthetic Mesh With Increased Stiffness," BJOG: Int. J. Obstet. Gynaecol., **120**(2), pp. 233–243.
[29] Goel, V. K., Lim, T. H., Gwon, J., Chen, J. Y., Winterbottom, J. M., Park, J. B., Weinstein, J. N., and Ahn, J. Y., 1991, "Effects of Rigidity of an Internal Fixation Device. A Comprehensive Biomechanical Investigation," Spine, **16**(3), pp. S155–S161.
[30] Jallah, Z., Liang, R., Feola, A., Barone, W., Palcsey, S., Abramowitch, S., Yoshimura, N., and Moalli, P., 2015, "The Impact of Prolapse Mesh on Vaginal Smooth Muscle Structure and Function," BJOG: Int. J. Obstet. Gynaecol., **123**(7), pp. 1076–1085.
[31] Rumian, A. P., Draper, E. R., Wallace, A. L., and Goodship, A. E., 2009, "The Influence of the Mechanical Environment on Remodelling of the Patellar Tendon," J. Bone Joint Surg. Br., **91**(4), pp. 557–564.

International Urogynecology Journal (2020) 31:91–99
https://doi.org/10.1007/s00192-019-04071-z

ORIGINAL ARTICLE

New Zealand white rabbit: a novel model for prolapse mesh implantation via a lumbar colpopexy

Katrina M. Knight[1,2] · Amanda M. Artsen[3] · Megan R. Routzong[4] · Gabrielle E. King[3] · Steven D. Abramowitch[3,4] · Pamela A. Moalli[3,4]

Received: 7 May 2019 / Accepted: 24 July 2019 / Published online: 15 August 2019

Abstract

Introduction and hypothesis New Zealand white rabbits are an inexpensive large-animal model. This study explored the rabbit as a model for mesh-augmented colpopexy using the intra-abdominal vagina. We hypothesized that polypropylene mesh would negatively impact rabbit vaginal smooth muscle (VSM) morphology and contractile function, similar to the nonhuman primate (NHP)—the established model for prolapse mesh evaluation.

Methods Restorelle was implanted onto the vagina of ten rabbits via lumbar colpopexy after a hysterectomy. Ten rabbits served as sham. Twelve weeks post-implantation, the vagina was excised and VSM morphology and vaginal contractility were assessed. Outcome measures were compared using independent samples t and Mann-Whitney U tests with a Bonferroni correction, where appropriate. Results from the rabbits were compared with published NHP data.

Results Animals had similar age, parity and BMI. VSM was 18% thinner after Restorelle implantation, $P = 0.027$. Vaginal contractility was 43% decreased in response to 120 mM KCl ($P = 0.003$), similar to the 46% reduction observed in the NHP vagina implanted with Restorelle ($P = 0.027$). Three meshes wrinkled in vivo, resulting in dramatic thinning of the underlying vagina in the area of the mesh causing a mesh exposure.

Conclusions Polypropylene mesh negatively impacts VSM morphology and vaginal contractility in the rabbit, similar to the NHP, suggesting that the rabbit may serve as an alternative large-animal model. The vaginal thinning and appearance of a mesh exposure in the area of a mesh wrinkle suggest the rabbit may also serve as a model for understanding the pathophysiology of mesh exposure.

Keywords New Zealand white rabbit · Vaginal smooth muscle · Pelvic organ prolapse · Modified abdominal sacrocolpopexy · Lumbar colpopexy · Polypropylene mesh

Introduction

Polypropylene mesh is commonly used in the surgical treatment of pelvic organ prolapse (POP) [1]. Unfortunately, mesh usage has been hampered by complications, with mesh exposure through the vaginal epithelium and pain most commonly reported [1]. The precise etiology of mesh complications is unclear. Animal models have improved our understanding of the impact of mesh on the vagina and provided insight into mechanisms of mesh complications [2–6].

The nonhuman primate (NHP), *Rhesus macaque*, is currently the gold standard model for investigating the impact of mesh on the vagina. NHPs are advantageous as they spontaneously develop prolapse and their pelvic anatomy and physiology are similar to those of humans [7]. Additionally, the NHP's pelvis is large enough to accommodate implantation of a prolapse mesh

Conference Presentation American Urogynecology Society 39th Annual Scientific Meeting, Chicago, IL, October 9–13, 2018

✉ Katrina M. Knight
kmk144@pitt.edu

[1] Department of Medicine, University of Pittsburgh, Pittsburgh, PA, USA

[2] Magee-Womens Research Institute, 204 Craft Avenue, Lab A320, Pittsburgh, PA 15213, USA

[3] Magee-Womens Research Institute, Department of Obstetrics and Gynecology and Reproductive Sciences at Magee Womens Hospital, University of Pittsburgh, Pittsburgh, PA, USA

[4] Department of Bioengineering, University of Pittsburgh, Pittsburgh, PA, USA

of reasonable dimensions onto the vagina in a flat configuration via an abdominal sacrocolpopexy (ASC), similar to humans. However, NHPs are a limited resource and are expensive, which limits the number and length of studies that can be conducted with this model. Hence, there is an urgent need for a cheaper large-animal model that can be used to investigate mechanisms of mesh complications.

The ewe is a cheaper and more accessible animal model relative to the NHP, and previous studies have utilized the ewe to implant mesh onto the vagina via a transvaginal approach [8–10]. However, performing abdominal surgery on ewes is surgically difficult because of the large rumen, and bowel obstructions are extremely common after surgery. The New Zealand White rabbit, on the other hand, is an alternative large-animal model that is cheaper than the NHP and is not a ruminant. Additionally, the rabbit vagina is large enough (~15 cm long and 2.5–4 cm wide) to allow for the implantation of mesh in a flat configuration. It is important to note that unlike in NHPs and humans, the rabbit vagina consists of two parts—an intra-abdominal portion and an external portion. The external vagina has previously been used for mesh implantation studies [11–15]. However, meshes implanted on the external vagina cannot be placed on tension because of limited accessibility of the pelvic side wall and spine. In contrast, mesh can be implanted in a flat configuration on the intra-abdominal vagina and placed on tension by attaching it to the spine, similar to an ASC. Additionally, compared with the external vagina, the intra-abdominal vagina is more representative of POP in women because it naturally lacks lateral and apical support, common sites of support defects in women with POP. In this way the rabbit may serve as an alternative model for addressing certain questions regarding the impact of mesh on the vagina such as the impact of tensioning and loading. We describe a novel method for implanting mesh onto the internal rabbit vagina and then define the impact of mesh on rabbit vaginal smooth muscle (VSM) morphology and vaginal contractility. Additionally, the results of this study were compared to the results from previous studies in which mesh was implanted onto the NHP vagina to assess the validity of using the rabbit as an alternative model to the NHP [4–6]. As studies utilizing the NHP have found that polypropylene mesh negatively impacts VSM morphology and vaginal contractility [4–6], we hypothesize the rabbit, if an appropriate model, would behave similarly.

Materials and methods

Animals

Twenty female New Zealand white rabbits, retired breeders, ages 2 to 3 years, were utilized according to experimental protocols approved by the University of Pittsburgh Institutional Animal Care and Use Committee (IACUC #16035431). Rabbits were housed in standard cages, on a 12-h alternating light/dark cycle, with water and a standard rabbit diet supplemented with hay and greens ad libitum.

Surgical procedures

Sterile samples (12×3 cm^2) of Restorelle (Coloplast, Minneapolis, MN) were implanted onto the anterior and posterior vagina via a modified ASC. Restorelle was chosen as it is widely used in humans and in previous studies had the least negative impact on vaginal morphology and function [4–6]. Following laparotomy, the bladder and rectum were gently dissected off of the vagina. Muscles overlying the lumbar spine were divided, and two 2-0 PDS II sutures, which served as the mesh-vagina anchoring sites, were placed through the ligamentous portion of the vertebral body. Next, a complete hysterectomy was performed without excision of the ovaries, and two straps of mesh were secured to the anterior and posterior vagina with 3-0 PDS II sutures. The two straps were then anchored to the lumbar spine with the previously placed 2-0 PDS II sutures (Fig. 1, right). For sham animals, the vagina with no mesh attached was anchored to the lumbar spine (Fig. 1, left). Lastly, the abdominal muscle layer was closed with 2-0 PDS II, and the skin was closed with a continuous subcuticular stitch (2-0 Vicryl). Note the more appropriate terminology for this modified ASC is lumbar colpopexy, a term that will be used throughout this manuscript. Twelve weeks post-implantation, the vagina with and without mesh was excised and harvested for histomorphology and biomechanical analyses.

Histology analysis

VSM morphology was assessed using Masson's trichrome staining. Briefly, full-thickness cross sections of the rabbit vagina with and without mesh were excised, fixed in formalin, embedded in paraffin and sectioned at 7 μm. Sections were stained with hematoxylin solution Gill no. 2 (to stain nuclei) and trichrome stain AB solution (Sigma-Aldrich, St. Louis, MO, USA) and imaged at ×100 using a Nikon Eclipse 90i imaging microscope (Melville, NY, USA). VSM thickness was measured using a custom Mathematica V11.3 (Wolfram, Champaign, IL) script, developed by Megan R. Routzong (co-author). Briefly, the smooth muscle layer was outlined by identifying the inner (i.e., the intersection where the sub-epithelium ends and the smooth muscle begins) and outer (i.e., the intersection where the smooth muscle ends and the adventitia begins) borders of the smooth muscle layer. The distance between the inner and outer border of the smooth muscle was then determined using built-in mathematical functions within Mathematica. This method was found to be within a 5% error when calculating the thickness of known geometries and manual measurements.

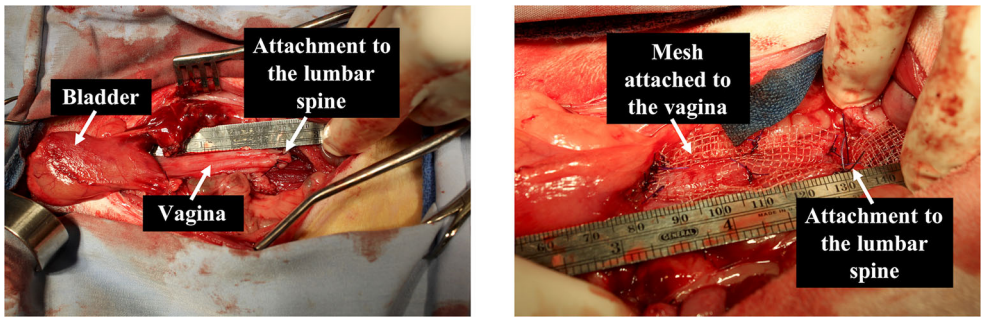

Fig. 1 Rabbit in vivo lumbar colpopexy. Surgical image depicting a lumbar colpopexy post-hysterectomy in which the vagina is attached to the lumbar spine without (left image) and with mesh attached to the vagina (right image). Note in the right image the mesh is attached to the vagina in a flat configuration.

Vaginal contractile function analysis

The contractile function of the VSM was assessed utilizing a vaginal contractility assay as previously described [4, 5]. Briefly, strips (approximately 7 mm × 2 mm) oriented along the circumferential direction were cut from the anterior and posterior proximal vagina (2 strips per side) with and without mesh. For samples with mesh, the mesh-vagina complex was tested intact to avoid damaging the tissue or the mesh and to afford testing of the contractile function of the vagina in the presence of mesh. Strips were clamped on opposing ends, and care was taken to ensure that no mesh was placed between the clamps in the case of mesh-implanted vaginas. Contraction of the vagina was induced using three stimulants: (1) 120 mM KCl to assess function of muscle myofibers via global muscle depolarization, (2) electrical field stimulation (EFS) 20 V for 5 s at 1–64 Hz to measure nerve-mediated smooth muscle contraction and (3) 10^{-7} to 10^{-4} M phenylephrine (an α_1-adreno-receptor agonist), applied non-cumulatively to measure receptor-mediated smooth muscle contraction via receptor depolarization. After each stimulant, maximum contractile force was recorded, and tissues were washed with Krebs solution prior to the application of the next stimulant. The resultant contractile forces generated in response to all three stimuli were normalized by the tissue volume. For comparison of rabbit to NHP, contractile force to EFS was also normalized by force generated in response to 120 mM KCl, both acceptable methods of normalization [4, 5, 16].

Historic nonhuman primate study design and analysis synopsis

Previously, Restorelle was implanted onto the anterior and posterior vaginal walls of eight middle-aged NHPs under nearly identical conditions—sacrocolpopexy after a hysterectomy with preservation of the ovaries [4–6]. Eight NHPs served as sham. Similar to the methods and analyses described previously, the histomorphology and thickness of the VSM were assessed after staining with Masson's trichrome and labeling with α-smooth muscle actin, respectively. The contractile function of the vagina was also evaluated using KCl and EFS as described for the rabbits. The NHP vagina does not consistently respond to phenylephrine; therefore, the response to phenylephrine was not compared between the rabbit and NHP. Given the similar methods utilized, the impact of mesh on VSM structure and vaginal contractility between the rabbit and NHP was compared.

Statistical analysis

Based on a power analysis, ten animals per group were needed to detect differences between groups with a power of 80% and a two-tailed significance set at $P < 0.05$. To determine whether the data were normally distributed, Kolmogorov-Smirnov tests were utilized. Differences in the smooth muscle thickness and contractile force within (rabbit sham vs. Restorelle) and between species (rabbit vs. nonhuman primate) were determined using independent samples t-tests in normally distributed data and Mann-Whitney U tests as a nonparametric alternative, with a Bonferroni correction where appropriate. All statistical analyses were performed utilizing SPSS 25.0 statistical software (IBM, Armonk, NY, USA).

Results

Twenty female rabbits underwent a hysterectomy with preservation of the ovaries followed by mesh implantation via lumbar colpopexy (a modified ASC) vs. sham (no mesh). One rabbit in the mesh-implanted group sustained a bowel obstruction and was excluded, leaving a final sample size of sham $N = 10$ and Restorelle $N = 9$. Animals had similar age and weight.

Gross morphology and histology analysis

At the time of tissue harvesting, vaginal tissue was well integrated within the pores of Restorelle in the mesh-implanted rabbit vagina (Fig. 2). Similar to humans and NHPs, the rabbit vagina had four layers (epithelium, subepithelium, muscularis and adventitia) (Fig. 3a) [7]. However, the rabbit vaginal epithelium is glandular, and the smooth muscle layer comprised approximately 70% of the overall thickness compared with approximately 30% of the NHP vagina (Fig. 3a and b). In six

Fig. 2 Mesh-vagina explant. Mesh-vagina complex explanted 12 weeks post lumbar colpopexy. Demonstrated in the image, vaginal tissue is incorporated between the pores of the mesh, and the mesh remained in the flat configuration in which it was implanted.

animals, meshes remained flat after implantation; however, three meshes wrinkled and were exposed through the vaginal epithelium (Fig. 4). In areas where the mesh wrinkled toward the vaginal lumen, there was an associated thinning of the underlying vagina (Fig. 5). This is in contrast to the meshes that remained flat after implantation, which displayed thinning of the muscularis without areas of extreme thinning as observed with wrinkles. Overall, the VSM layer was significantly thinner after Restorelle implantation compared with sham [1577.1 (319.4) μm vs. 1286.8 (125.0) μm, respectively (P = 0.027)].

Contractile function

The contractile function of the rabbit vagina without and with mesh implanted was assessed utilizing 120 mM KCl, EFS and phenylephrine. Given that anterior and posterior strips of the vagina were evaluated, statistical analyses were performed to determine whether the contractile function of the sham anterior and posterior strips of the vagina differed. In response to all three stimuli, the resulting contractile forces were not significantly different between the sham anterior and posterior vagina (120 mM KCl $P = 0.518$, EFS $P = 0.428$ and phenylephrine $P = 0.114$); therefore, for the purposes of this study, the contractility data presented here represent the average contractile force of the anterior and posterior vagina.

Implanting Restorelle onto the rabbit vagina negatively impacted the ability of the myofibers, nerves and receptors to induce a smooth muscle contraction (Table 1). The contractile force decreased 43.3% in response to 120 mM KCl (P = 0.003), 50% following EFS ($P = 0.007$) and 44.9% following stimulation with phenylephrine ($P = 0.012$). A similar 46.2% decrease in muscle-mediated contractile function was observed with the implantation of Restorelle onto the NHP vagina, $P = 0.027$; however, nerve-medicated contractile function was not significantly decreased ($P = 0.379$), and a contractile response to phenylephrine was not consistently observed, likely because of the higher smooth muscle content in the rabbit vagina.

Compared with the nonhuman primate, the rabbit vagina was significantly more contractile (Table 2). In response to 120 mM KCl, the rabbit vagina, without (sham) and with mesh implanted (Restorelle), was 6.6- ($P < 0.001$) and 6.9- ($P < 0.001$) fold more contractile than the NHP sham and Restorelle-implanted vagina, respectively. Similarly, the rabbit vagina without (sham) and with mesh implanted

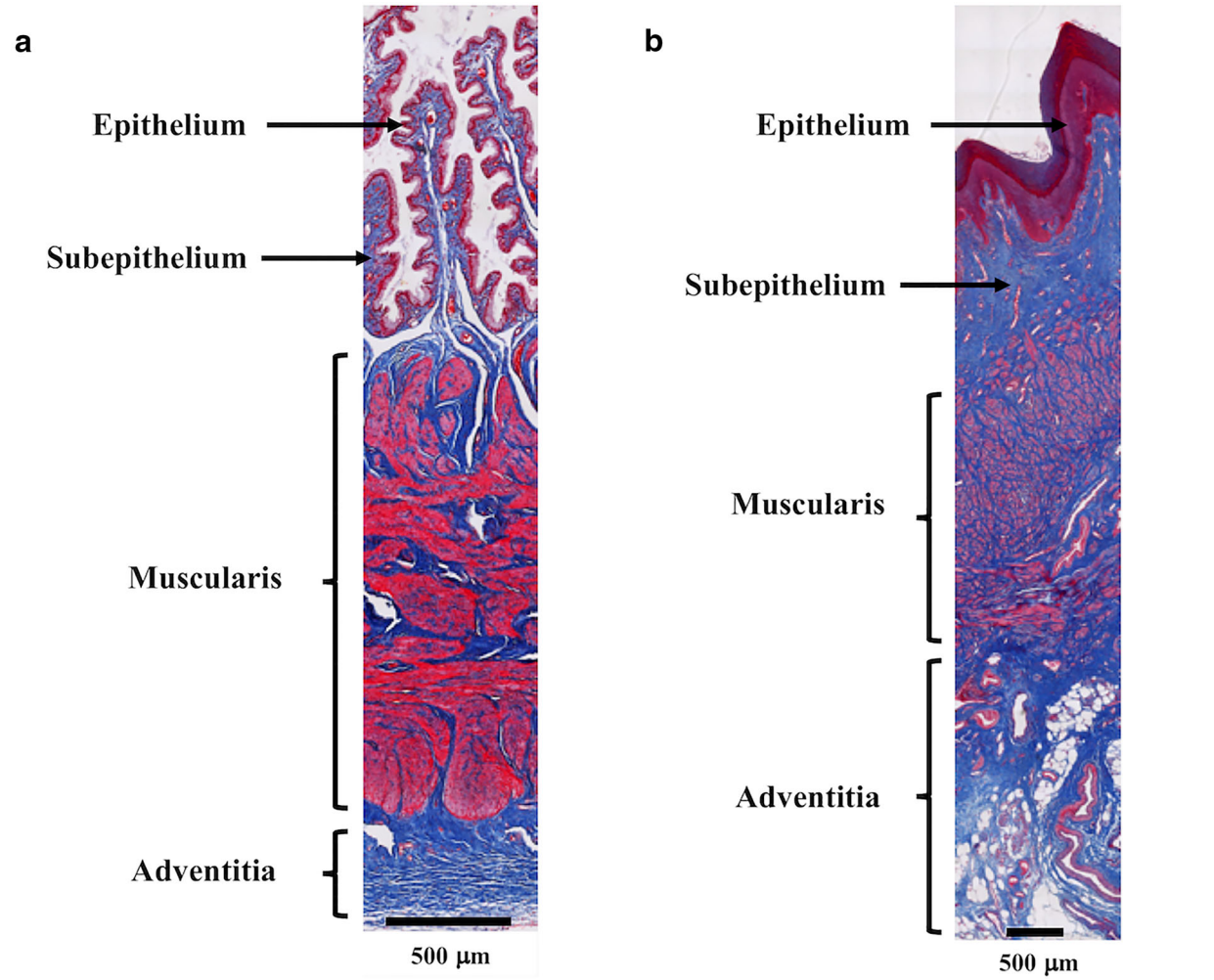

Fig. 3 Rabbit and nonhuman primate sham vaginal cross section. Masson's trichrome staining of the **a** rabbit and **b** nonhuman primate sham vagina demonstrating the characteristic layers of the vagina with a prominent muscularis (smooth muscle) layer. Relative to the nonhuman primate, the muscularis layer makes up a greater portion of the rabbit vagina.

(Restorelle) was 88- and 44- fold more contractile than the NHP sham and Restorelle-implanted vagina in response to EFS, respectively ($P < 0.001$ for both). Normalizing the contractile force to EFS by the contractile force in response to 120 mM KCl, an alternative method of normalization, resulted in a similar decrease in smooth muscle contractility in the rabbit and NHP sham vagina ($P = 0.315$). The decrease in contractility between the rabbit and NHP Restorelle-implanted vagina was also similar by this method ($P = 0.610$).

Discussion

By suspending the vagina to the lumbar spine via a mesh bridge (lumbar colpopexy), we were able to (1) implant Restorelle onto the rabbit internal vagina in a flat configuration and (2) recreate the loading conditions observed during a human ASC. Interestingly, the internal vagina of the rabbit lacks lateral and apical support structures and therefore is similar to the vagina of women with advanced prolapse. The most important points of this study are that, first, implanting polypropylene mesh onto the rabbit internal vagina resulted in a significant decrease in VSM thickness and vaginal contractile function, similar to previous observations following implantation of Restorelle in the NHP. This finding is congruent with the study hypothesis and suggests that the rabbit can serve as an alternative model to the NHP. Second, significant thinning of the vagina was observed in areas where the mesh wrinkled, similar to what is seen in women with mesh exposure. In this way, the rabbit is one of the first models with potential for directly studying the mechanism(s) of mesh exposure. The third major finding was the rabbit vagina is comprised of considerably more muscle than the NHP (or human based on qualitative observation) and appears more sensitive to VSM stimulants, suggesting that it might also be a preferred model for studying the impact of vaginal implants on VSM.

VSM thickness significantly decreased with the implantation of mesh for the rabbit but not for the NHP, although the

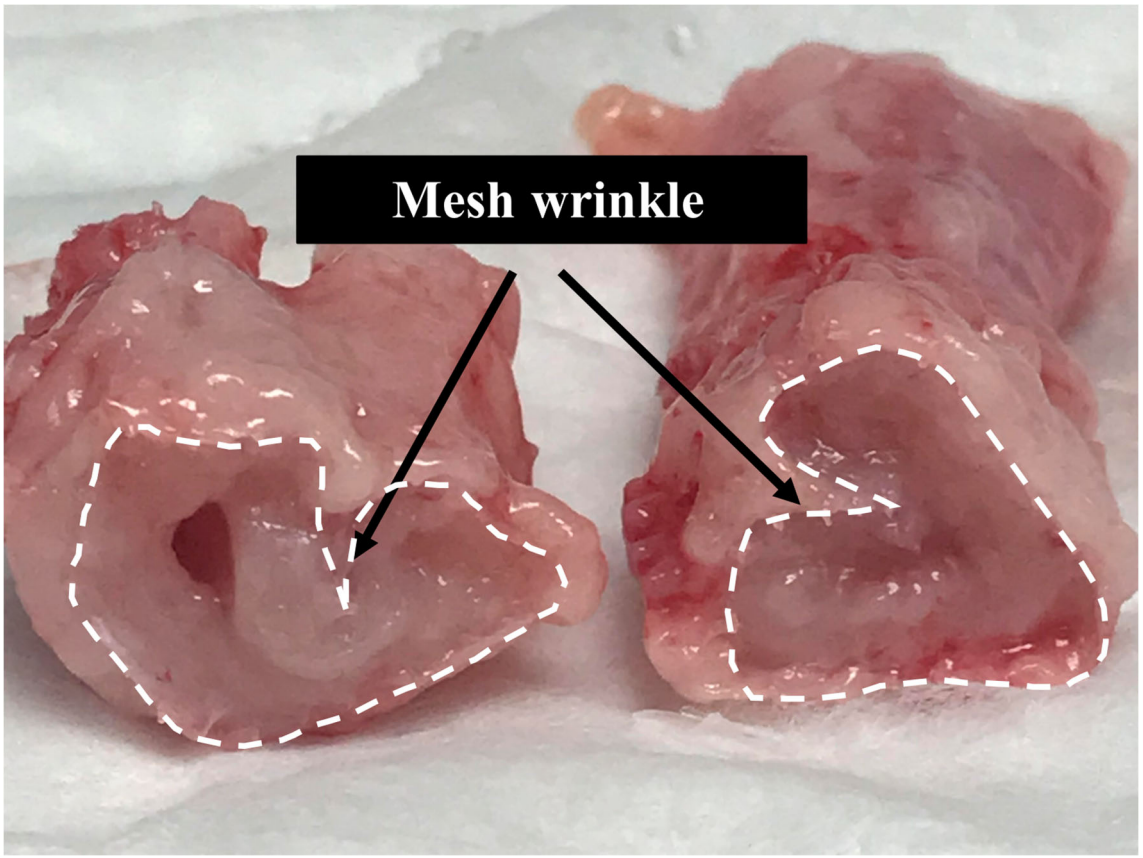

Fig. 4 Mesh wrinkle. Cross-sectional view of the mesh-vagina complex depicting a mesh wrinkle.

trend was similar. This is likely a result of the rabbit vagina consisting of proportionally more smooth muscle than the NHP in which the smooth muscle layer is not as predominant. Hence, changes in thickness will be more observable in the rabbit VSM than in the NHP. The relative change in the contractile force in response to EFS for the rabbit was higher than the NHP, 50% and 31%, respectively, and only the decrease in the rabbit achieved statistical significance. However, when normalizing the EFS contractile force by the force of contraction to 120 mM KCl, the observed decrease in both

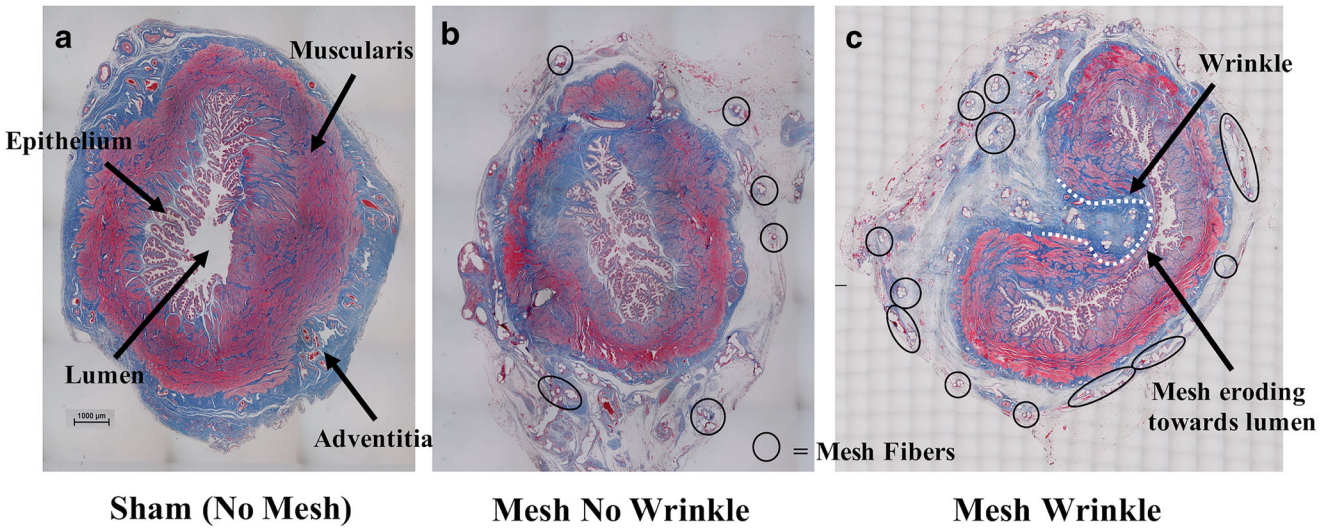

Fig. 5 Smooth muscle thinning with mesh implantation. Cross-sectional images of the rabbit vagina stained with Masson's trichrome staining depicting: **a** a vagina in which no mesh was implanted, **b** a mesh with no wrinkle and **c** a mesh wrinkle in which the mesh fibers (black circles) erode toward the lumen (dotted white line) of the vagina (characteristic of a mesh exposure). Overall, thinning of the muscularis (smooth muscle) layer was observed in the mesh-implanted rabbit vagina relative to sham. Note: For esthetics, only a few mesh fibers are outlined in **b** and **c**.

Table 1 Rabbit maximum contractile force in response to stimuli

Stimulant	Sham ($N = 10$)	Restorelle ($N = 9$)	P value
120 mM Potassium chloride (mN/mm^3)	1.71 ± 0.52	0.97 ± 0.41	0.003[a]
Electrical field stimulation (mN/mm^3)	0.88 (1.10)	0.44 (0.43)	0.007[b]
Phenylephrine (mN/mm^3)	2.36 ± 0.89	1.30 ± 0.74	0.012[a]

Data represented as mean ± standard deviation or median (interquartile range)

[a] P value obtained using independent samples t-test

[b] P value obtained using Mann-Whitney U test

models was statistically similar, suggesting that the impact of mesh on nerve-mediated contractions is indeed similar for the rabbit and NHP. Likewise, the relative change in the muscle-mediated contractions was significantly decreased for both rabbit (43% decreased) and NHP (46% decreased). Together these results support that the impact of polypropylene mesh on the rabbit and NHP vagina is similar.

Vaginal smooth muscle plays an essential role in maintaining vaginal tone and the overall support of the vagina through the connection between VSM fibers and fibers of the levator ani muscles [17]. Additionally, VSM is critical to sexual function as the relaxation of VSM with sexual stimulation results in vaginal enlargement, vasocongestion, engorgement and lubrication [18]. Studies have shown that in women with POP, VSM is disorganized, the fractional area of smooth muscle is decreased, and smooth muscle apoptosis is increased [19–21]. Based on studies in the NHP and now the rabbit demonstrating the negative impact of polypropylene mesh on VSM, it is possible that surgeons are implanting mesh onto a vagina that is already compromised with regard to VSM structure and function and that mesh could be exacerbating this condition. With the abundance of VSM within the rabbit and the ability to elicit both nerve- and receptor-mediated contractions, the rabbit model provides a cost-effective model for defining the impact of mesh on VSM morphology and function.

Mesh exposure is one of the most common complications reported, occurring in approximately 10–20% of the meshes placed transvaginally and 10.5% of meshes placed transabdominally with rates that increase with time [1, 22–25]. Infection, host reaction to a foreign material, stress mis-matches between the mesh and the vagina, and micro-motion are all proposed mechanisms [2, 4, 6]. Clinically, mesh exposures are often observed in the areas of a mesh wrinkle and/or contraction [26, 27]. Furthermore, mesh explants removed from women with exposure demonstrate marked deformation and wrinkling associated with increased pro-MMP-9 and cytotoxic T cells relative to control tissue without mesh, indicative of tissue degradation [28, 29]. Indeed, thinning of the underlying tissue in the area of mesh wrinkles, as observed in this study, strongly suggests that mesh wrinkling leading to tissue degradation is a plausible mechanism for mesh exposure.

Together, our data establishing the rabbit model as an alternative to the NHP comprise a crucial next step toward understanding mechanisms of mesh complications, particularly those whose pathophysiology involves smooth muscle dysfunction and atrophy. The availability, size, ability to implant mesh via a lumbar colpopexy and relatively low expense of the rabbit give scientists the ability to investigate multiple research questions and to conduct long-term studies.

The strengths of this study include the use of an inexpensive large-animal model that lacks apical and lateral vaginal support similar to women with POP. Additionally, the methods utilized to assess the contractile function of the rabbit vagina are the same as those used previously for the NHP and women with prolapse, which allows for a direct comparison between species [4, 5, 30]. The NHP ASC model also served as a way to validate the rabbit lumbar colpopexy model

Table 2 Rabbit vs. nonhuman primate contractile force response to stimuli

Stimulant	Sham			Restorelle		
	Rabbit ($N = 10$)	NHP ($N = 8$)	Rabbit vs. NHP	Rabbit ($N = 9$)	NHP ($N = 8$)	Rabbit vs. NHP
120 mM Potassium chloride (mN/mm^3)	1.71 ± 0.52	0.26 ± 0.11	P value < 0.001[b]	0.97 ± 0.41	0.14 ± 0.08	P value < 0.001[b]
Electrical field stimulation (mN/mm^3)	0.88 (1.10)	0.01 (0.02)	P value < 0.001[b]	0.44 (0.43)	0.01 (0.02)	P value < 0.001[b]
Electrical field stimulation (g/g)	0.46 (0.69)	0.46 (0.44)	$P = 0.315$[b]	0.51 (0.36)	0.62 (0.49)	$P = 0.610$[a]

NHP nonhuman primate

Data represented as mean ± standard deviation or median (interquartile range)

[a] P value obtained using independent samples t-test

[b] P value obtained using Mann-Whitney U test

developed in this study. This study however has some limitations which must be considered. First, the rabbit vagina is structurally different from that of humans. Specifically, the rabbit vagina has a glandular epithelium, it is primarily smooth muscle and is thinner than the human vagina (which can make the rabbit vagina more susceptible to mesh complications), and it lacks lateral and apical support (typical of women with POP but not women with normal support). Furthermore, the rabbit is a quadruped and it does not develop POP spontaneously. Due to the inherent challenges in conducting longitudinal experiments on tissue in women undergoing prolapse procedures, researchers must utilize animal models that mimic the human condition. Indeed, if the appropriate animal model is chosen based on the research question investigated, the limitations of utilizing an animal model can be reduced. Second, the contractile function of the VSM from sham and Restorelle-implanted animals was indirectly measured with the vagina or mesh-vagina complex completely intact (i.e., the VSM was not isolated from the other layers of the vagina). This was done to (1) avoid any damage that would occur when separating the smooth muscle layer from the other layers of the vagina, especially since the mesh was well integrated within the vaginal tissue, and (2) to determine how vaginal tissue functions (i.e., contracts) in the presence of mesh. In this study, the contractile function reported was normalized to the volume of the sample tested to account for any differences in the dimensions of the samples (e.g., length, width and thickness). This addresses questions about the overall contractile function of the organ as a whole, but does not provide information on the contractile phenotype of specific cells or cell layers. Lastly, stimulating rabbit vaginal tissue with 120 mM KCl did not produce the maximal contractile response (i.e., phenylephrine stimulation produced the highest response in this study), but did allow for a direct comparison to that of the NHP since 120 mM KCl was also utilized on the NHP vagina. Moreover, we performed a preliminary dose-response curve of the rabbit vagina (the smooth muscle was not isolated from the other layers of the vagina) in response to KCl and found that the dose for maximal stimulation (over 160 mM KCl) substantially exceeds physiologic ranges.

Overall, this study demonstrated that polypropylene mesh negatively impacts rabbit vaginal morphology and function, similar to what we have observed in the NHP, suggesting that the rabbit model can serve as an alternate model. Perhaps most interestingly and unexpectedly, we were able to recreate conditions consistent with mesh exposures in women. In this way, the rabbit may serve as a model for understanding the mechanism(s) of mesh exposure.

Acknowledgments We are grateful for the financial support from the Department of Defense (DOD) (grant no. W81XWH-16-1-0133). The DOD did not provide any assistance with the study design, the collection, analysis and interpretation of data or in the writing of this report or in the decision to submit the article for publication. Research reported in this publication was also supported by the National Center for Advancing Translational Sciences of the National Institutes of Health under award no. TL1TR001858. The content is solely the responsibility of the authors and does not necessarily represent the official views of the National Institutes of Health. The authors would like to thank Dr. Naoki Yoshimura MD, PhD (Professor of Urology, Pharmacology, and Cell Biology, University of Pittsburgh), for allowing us to use the organ bath system to collect the contractility data reported and Stacy Palcsey for her assistance with this study.

Funding This study was funded by the Department of Defense (grant no. W81XWH-16-1-0133) and the National Center for Advancing Translational Sciences of the National Institutes of Health (award no. TL1TR001858).

Compliance with ethical standards

Conflicts of interest None.

References

1. FDA. Surgical mesh for treatment of women with pelvic organ prolapse and stress urinary incontinence: FDA executive summary. 2011.
2. Brown BN, Mani D, Nolfi AL, Liang R, Abramowitch SD, Moalli PA. Characterization of the host inflammatory response following implantation of prolapse mesh in rhesus macaque. Am J Obstet Gynecol. 2015;213(5):668e661–10. https://doi.org/10.1016/j.ajog.2015.08.002.
3. Endo M, Feola A, Sindhwani N, Manodoro S, Vlacil J, Engels AC, et al. Mesh contraction: in vivo documentation of changes in apparent surface area utilizing meshes visible on magnetic resonance imaging in the rabbit abdominal wall model. Int Urogynecol J. 2014:1–7.
4. Feola A, Abramowitch S, Jallah Z, Stein S, Barone W, Palcsey S, et al. Deterioration in biomechanical properties of the vagina following implantation of a high-stiffness prolapse mesh. BJOG Int J Obstet Gynaecol. 2013;120(2):224–32.
5. Jallah Z, Liang R, Feola A, Barone W, Palcsey S, Abramowitch S, et al. The impact of prolapse mesh on vaginal smooth muscle structure and function. BJOG Int J Obstet Gynaecol. 2015. https://doi.org/10.1111/1471-0528.13514.
6. Liang R, Abramowitch S, Knight K, Palcsey S, Nolfi A, Feola A, et al. Vaginal degeneration following implantation of synthetic mesh with increased stiffness. BJOG Int J Obstet Gynaecol. 2013;120(2):233–43.
7. Abramowitch SD, Feola A, Jallah Z, Moalli PA. Tissue mechanics, animal models, and pelvic organ prolapse: a review. Eur J Obstet Gynecol Reprod Biol. 2009;144(SUPPL 1):S146–58.
8. Endo M, Urbankova I, Vlacil J, Sengupta S, Deprest T, Klosterhalfen B, et al. Cross-linked xenogenic collagen implantation in the sheep model for vaginal surgery. Gynecol Surg. 2015;12(2):113–22. https://doi.org/10.1007/s10397-015-0883-7.
9. Feola A, Endo M, Urbankova I, Vlacil J, Deprest T, Bettin S, et al. Host reaction to vaginally inserted collagen containing polypropylene implants in sheep. Am J Obstet Gynecol. 2015;212(4):474.e471–8. https://doi.org/10.1016/j.ajog.2014.11.008.
10. Tayrac R, Alves A, Thérin M. Collagen-coated vs noncoated low-weight polypropylene meshes in a sheep model for vaginal surgery. A pilot study. Int Urogynecol J. 2007;18(5):513–20. https://doi.org/10.1007/s00192-006-0176-9.

11. Fan X, Wang Y, Wang Y, Xu H. Comparison of polypropylene mesh and porcine-derived, cross-linked urinary bladder matrix materials implanted in the rabbit vagina and abdomen. Int Urogynecol J. 2014;25(5):683–9. https://doi.org/10.1007/s00192-013-2283-8.
12. Hilger WS, Walter A, Zobitz ME, Leslie KO, Magtibay P, Cornella J. Histological and biomechanical evaluation of implanted graft materials in a rabbit vaginal and abdominal model. Am J Obstet Gynecol. 2006;195(6):1826–31. https://doi.org/10.1016/j.ajog.2006.07.006.
13. Pierce LM, Grunlan MA, Hou Y, Baumann SS, Kuehl TJ, Muir TW. Biomechanical properties of synthetic and biologic graft materials following long-term implantation in the rabbit abdomen and vagina. Am J Obstet Gynecol. 2009;200(5):549.e541–8. https://doi.org/10.1016/j.ajog.2008.12.041.
14. Pierce LM, Rao A, Baumann SS, Glassberg JE, Kuehl TJ, Muir TW. Long-term histologic response to synthetic and biologic graft materials implanted in the vagina and abdomen of a rabbit model. Am J Obstet Gynecol. 2009;200(5):546.e541–8. https://doi.org/10.1016/j.ajog.2008.12.040.
15. Huffaker RK, Muir TW, Rao A, Baumann SS, Kuehl TJ, Pierce LM. Histologic response of porcine collagen-coated and uncoated polypropylene grafts in a rabbit vagina model. Am J Obstet Gynecol. 2008;198(5):582.e581–7. https://doi.org/10.1016/j.ajog.2007.12.029.
16. Skoczylas LC, Jallah Z, Sugino Y, Stein SE, Feola A, Yoshimura N, et al. Regional differences in rat vaginal smooth muscle contractility and morphology. Reproductive sciences (Thousand Oaks, Calif). 2013;20(4):382–90. https://doi.org/10.1177/1933719112472733.
17. DeLancey JOL, Starr RA. Histology of the connection between the vagina and levator ani muscles. Implications for urinary tract function. Journal of Reproductive Medicine for the Obstetrician and Gynecologist. 1990;35(8):765–71.
18. Goldstein I, Alexander JL. Practical aspects in the management of vaginal atrophy and sexual dysfunction in perimenopausal and postmenopausal women. J Sex Med. 2005;2:154–65. https://doi.org/10.1111/j.1743-6109.2005.00131.x.
19. Boreham MK, Wai CY, Miller RT, Schaffer JI, Word RA. Morphometric analysis of smooth muscle in the anterior vaginal wall of women with pelvic organ prolapse. Am J Obstet Gynecol. 2002;187(1):56–63. https://doi.org/10.1067/mob.2002.124843.
20. Boreham MK, Wai CY, Miller RT, Schaffer JI, Word RA, Weber A. Morphometric properties of the posterior vaginal wall in women with pelvic organ prolapse. Am J Obstet Gynecol. 2002;187(6):1501–9. https://doi.org/10.1067/mob.2002.130005.
21. Takacs P, Gualtieri M, Nassiri M, Candiotti K, Medina CA. Vaginal smooth muscle cell apoptosis is increased in women with pelvic organ prolapse. Int Urogynecol J Pelvic Floor Dysfunct. 2008;19(11):1559–64. https://doi.org/10.1007/s00192-008-0690-z.
22. Halaska M, Maxova K, Sottner O, Svabik K, Mlcoch M, Kolarik D, et al. A multicenter, randomized, prospective, controlled study comparing sacrospinous fixation and transvaginal mesh in the treatment of posthysterectomy vaginal vault prolapse. Am J Obstet Gynecol. 2012;207(4):301.e301–7. https://doi.org/10.1016/j.ajog.2012.08.016.
23. Jacquetin B, Hinoul P, Gauld J, Fatton B, Rosenthal C, Clavé H, et al. Total transvaginal mesh (TVM) technique for treatment of pelvic organ prolapse: a 5-year prospective follow-up study. Int Urogynecol J. 2013;24(10):1679–86. https://doi.org/10.1007/s00192-013-2080-4.
24. Nieminen K, Hiltunen R, Takala T, Heiskanen E, Merikari M, Niemi K, et al. Outcomes after anterior vaginal wall repair with mesh: a randomized, controlled trial with a 3 year follow-up. Am J Obstet Gynecol. 2010;203(3):235.e231–8. https://doi.org/10.1016/j.ajog.2010.03.030.
25. Nygaard I, Brubaker L, Zyczynski HM, Cundiff G, Richter H, Gantz M, et al. Long-term outcomes following abdominal sacrocolpopexy for pelvic organ prolapse. JAMA. 2013;309(19):2016–24. https://doi.org/10.1001/jama.2013.4919.
26. Feiner B, Maher C. Vaginal mesh contraction: definition, clinical presentation, and management. Obstet Gynecol. 2010;115(2 PART 1):325–30.
27. Svabik K, Martan A, Masata J, El-Haddad R, Hubka P, Pavlikova M. Ultrasound appearances after mesh implantation—evidence of mesh contraction or folding? Int Urogynecol J. 2011;22(5):529–33. https://doi.org/10.1007/s00192-010-1308-9.
28. Nolfi AL, Brown BN, Liang R, Palcsey SL, Bonidie MJ, Abramowitch SD, et al. Host response to synthetic mesh in women with mesh complications. Am J Obstet Gynecol. 2016;215(2):206.e201–8. https://doi.org/10.1016/j.ajog.2016.04.008.
29. Tennyson L, Rytel M, Palcsey S, Meyn L, Liang R, Moalli P. Characterization of the T cell response to polypropylene mesh in women with complications. Am J Obstet Gynecol. 2018. https://doi.org/10.1016/j.ajog.2018.11.121.
30. Northington GM, Basha M, Arya LA, Wein AJ, Chacko S. Contractile response of human anterior vaginal muscularis in women with and without pelvic organ prolapse. Reprod Sci. 2011;18(3):296–303. https://doi.org/10.1177/1933719110392054.